

Review of magnetic properties and magnetocaloric effect in the intermetallic compounds of rare earth with low boiling point metal(s)*

Li Ling-Wei (李领伟)[†]

Key Laboratory of Electromagnetic Processing of Materials (Ministry of Education), Northeastern University, Shenyang 110819, China

Abstract: The magnetocaloric effect (MCE) in many rare earth (*RE*) based intermetallic compounds has been extensively investigated during last two decades, not only due to their potential applications for magnetic refrigeration but also for better understanding of the fundamental problems of the materials. This paper reviews our recent progress of magnetic properties and MCE in some binary or ternary intermetallic compounds of *RE* with low boiling point metal(s) (Zn, Mg, and Cd). Some of them are exhibiting promising MCE properties which make them also attractive for low temperature magnetic refrigeration. Characteristics of the magnetic transition, origin of large MCE as well as the potential application of these compounds were thoroughly discussed. Additionally, a brief review of the magnetic and magnetocaloric properties in the quaternary rare earth nickel boroncarbides $RENi_2B_2C$ superconductors is also presented.

Keywords: Magnetocaloric effect; Rare earth based intermetallic compounds; Low boiling point metal(s); $RENi_2B_2C$ superconductors; Magnetic phase transition

* Project supported by the National Natural Science Foundation of China (Nos. 11374081 and 11004044), the Fundamental Research Funds for the Central Universities (Grant Nos. L1509006 and N140901001), the Japan Society for the Promotion of Science Postdoctoral Fellowships for Foreign Researchers (No. P10060), and the Alexander von Humboldt (AvH) Foundation (Research stipend to L. Li). I sincerely thank Prof. Rainer Pöttgen from Universität Münster, Germany and Prof. Katsuhiko Nishimura from University of Toyama, Japan for the fruitful discussions and helpful suggestions.

[†] Author to whom correspondence should be addressed. Electronic mail: lingwei@epm.neu.edu.cn (Lingwei Li), wei0396@hotmail.com (Lingwei Li); Tel. +86-24-83684653.

1. Introduction of magnetocaloric effect and materials

The magnetocaloric effect (MCE) is a magneto-thermodynamic phenomenon which was first discovered in pure Fe by Emil Warburg in 1881,^[1] and its origin was independently explained by Debye and Giaque in the 1920s.^[2, 3] All magnetic materials exhibit MCE, although the intensity of this effect depends on the properties of each material. Generally, for a simple ferromagnetic material near its Curie temperature, when a magnetic field is applied, the spins tend to align parallel to the magnetic field which lowers the magnetic entropy. To compensate for the loss in the magnetic entropy in an adiabatic (isentropic) process the temperature of the material increases. When the magnetic field is removed, the spins tend to become random which increases the magnetic entropy and the material cools. Meanwhile, Debye and Giaque have also proposed the adiabatic demagnetization in order to achieve temperature lower than that of the liquid helium. This possibility was later experimentally demonstrated by the chemist Nobel Laureate William F. Giaque in 1933, he was able to reach a temperature of 0.25 K based on the adiabatic demagnetization of 61g paramagnetic salts $Gd_2(SO_4)_3 \cdot 8H_2O$.^[4] Besides the success in the ultralow temperature, the magnetic refrigeration technology has also been applied at the higher temperature ranges, such as ~2 to 20 K, the range of liquid helium and hydrogen, as well as ~20 to 80 K, the range of liquid hydrogen and nitrogen.^[5-8]

In 1997, two key developments enhanced the feasibility for producing a magnetic refrigerator for commercial or industrial use. The first is that Zimm et al^[9] realized the first near room temperature magnetic refrigeration prototype at the Ames Laboratory. Second is that Pecharsky and Gschneider^[10] observed a giant MCE in the $Gd_5(Si_2Ge_2)$ compound. Besides the discovery of the giant MCE in $Gd_5(Si_2Ge_2)$ and related compounds,^[10, 11] a number of materials with giant/large MCE have been realized in last three decades, for example $RECo_2$ ($RE = Er, Ho$,

and Dy) alloys,^[12, 13] MnAs based compounds,^[14-17] manganites $(RE,M)MnO_3$, (RE = lanthanide, M = Ca, Sr, and Ba),^[18,19] Ni-Mn-X (X = Ga, In, and Sn) based Heusler alloys,^[20-24] $La(Fe,Si)_{13}$ and related compounds,^[25-28] $MnTX$ (T = Co, Ni, and Fe; X = Si, Ge) based compounds^[29-32] as well as some rare earth (RE) based intermetallic compounds.^[33-36] The structure, physical properties as well as the MCE and its application in most of the above mentioned materials have been summarized in a number of reviews articles ^[11-14, 17-19, 22, 23, 26, 27, 32-35, 37-40] which will not be repeated here. In this paper, we give a brief review of our recent progress in exploring magnetocaloric materials, mainly related to several typical systems of RE -based intermetallic compounds.

2. Characterization of magnetocaloric materials

2.1. Evaluation of magnetic entropy change (ΔS_M) and adiabatic temperature change (ΔT_{ad})

The MCE is an intrinsic phenomenon for magnetic materials which manifests as the isothermal magnetic entropy change ΔS_M or/and the adiabatic temperature change ΔT_{ad} when it is exposed to a varying magnetic field, the definition of ΔS_M and ΔT_{ad} can be found in Fig. 1. The MCE can be measured directly or it can be calculated indirectly from the experimentally measured heat capacity and/or magnetization. In the present review, the reported values of ΔS_M and ΔT_{ad} were estimated from two different methods using the indirect technology: (1) from field and temperature dependence of heat capacity $C(H, T)$, (2) from field and temperature dependence of magnetization $M(H, T)$ and zero field heat capacity $C(T, 0T)$ which were described as below:

The temperature dependence of total entropy S under different fields can be calculated from

heat capacity by numerical integration:

$$S(H, T) = \int_0^T \left(\frac{C(H, T)}{T} \right)_H dT \quad (1)$$

where H is the magnetic field at which the heat capacity was measured. Then the ΔS_M as well as the adiabatic temperature change ΔT_{ad} can be calculated from the heat capacity measurements using the following relations:

$$\Delta S_M(T, \Delta H) = \int_0^T \frac{C(T, H_1) - C(T, H_0)}{T} dT = [S(T)_{H_1} - S(T)_{H_0}]_T, \quad (2)$$

$$\Delta T_{ad}(\Delta H, T) = [T(S)_{H_1} - T(S)_{H_0}]_S. \quad (3)$$

According to thermodynamical theory, the isothermal magnetic entropy changes associated with a magnetic field variation is given by

$$\Delta S_M(T, \Delta H) = S_M(T, H_1) - S_M(T, H_0) = \int_0^H \left(\frac{\partial S(H, T)}{\partial H} \right)_T dH \quad (4)$$

From the Maxwell's thermodynamic relation:

$$\left(\frac{\partial S(H, T)}{\partial H} \right)_T = \left(\frac{\partial M(H, T)}{\partial T} \right)_H, \quad (5)$$

one can obtain the following expression:

$$\Delta S_M(T, \Delta H) = \int_0^H \left(\frac{\partial M(H, T)}{\partial T} \right)_H dH \quad (6)$$

where S , M , H , and T are the magnetic entropy, magnetization of the material, applied magnetic field, and the temperature of the system, respectively. From the magnetization measurements made at discrete field and temperature intervals, ΔS_M can be approximately calculated by the following expression:

$$\Delta S_M(T, \Delta H) \approx \frac{1}{\delta T} \left[\int_0^H M(T + \delta T, H) dH - \int_0^H M(T, H) dH \right]. \quad (7)$$

From zero field $C(T)$, we can calculate $S(T, 0 T)$ by using equation 1. Using the magnetic entropy change ΔS_M calculated from $M(H, T)$, the $S(T, H)$ can be calculated from the following expression:

$$S(T, H_1) = \Delta S_M(T, \Delta H) + \int_0^T \left(\frac{C(T, H_0)}{T} \right)_H dT. \quad (8)$$

Then the adiabatic temperature change ΔT_{ad} can be calculated using Eq. 3. Using the present method, the accuracy of the ΔS_M calculated from the magnetization data for the materials studied here is better than 10%.

2.2. Evaluation of the relative cooling power (RCP) and refrigerant capacity (RC)

Another important quality factor(s) for magnetocaloric materials is the relative cooling power (RCP) or/and refrigerant capacity (RC) which is a measurement of the amount of heat transfer between the cold and hot reservoirs in an ideal refrigeration cycle. The RCP is defined as the product of the maximum magnetic entropy change $-\Delta S_M^{\max}$ and full width at half maximum, δT_{FWHM} , in $\Delta S_M(T)$ curve,

$$i.e., RCP = -\Delta S_M^{\max} \times \delta T^{FWHM}. \quad (9)$$

Whereas, the RC is calculated by numerically integrating the area under the $-\Delta S_M$ - T curve at half maximum of the peak taken as the integration limits, where T_1 and T_2 are the temperatures of the cold end and the hot end of an ideal thermodynamic cycle, respectively,

$$i.e., RC = \int_{T_1}^{T_2} |\Delta S_M| dT. \quad (10)$$

An example for the evaluation of the RCP and RC is displayed in Fig. 2. It is easy to find that the value of RC is around 25 % lower than that of the RCP for the $\Delta S_M(T)$ that with a single broad triangle peak around T_C , which is a typical character for the second order MCE materials.

2.3. Determination of the order of magnetic phase transition

It is well known that the magnitude, temperature and magnetic field change dependence of MCE have strong correlation with the nature of the corresponding magnetic phase transition; therefore, it is important to determine the order of magnetic transition of the magnetocaloric materials. Based on the Inoue-Shimizu model,^[41, 42] which involves a Landau expansion of the magnetic free energy up to sixth power of the total magnetization M , can be used to determine the magnetic transition type,^[41,42]

$$F(M, T) = \frac{c_1(T)}{2} M^2 + \frac{c_2(T)}{4} M^4 + \frac{c_3(T)}{6} M^6 + \dots - BM. \quad (11)$$

After minimization of the above equation with respect to the magnetization M , the magnetization near the Curie temperature T_C :

$$c_1(T)M + c_2(T)M^3 + c_3(T)M^5 = B. \quad (12)$$

The parameters $c_1(T)$, $c_2(T)$ and $c_3(T)$ represent the Landau coefficient, and it has been reported that the order of a magnetic transition is related to the sign of the $c_2(T)$. A transition is expected to be the first order when $c_2(\sim T_C)$ is negative, whereas it will be the second order for a positive $c_2(\sim T_C)$. The sign of c_2 can be determined by Arrott plot (H/M versus M^2 curves)^[43], *i. e.* the magnetic transition is of second order if all the H/M versus M^2 curves have positive slope. On the other hand, if the H/M versus M^2 curves show negative slope, the magnetic transition is of the first order. In the present review, the order of magnetic phase transition of all the materials was determined by this method.

3. MCE in rare earth based intermetallic compounds that contains low boiling point metal(s)

The rare earth (*RE*) – transition metal (*T*) based systems have intensively been investigated in recent years with respect to their interesting chemical and physical properties as well as practical applications in a wide spectrum of industries. Depending on the constituent element and composition, various properties like magnetic ordering, superconductivity, heavy-fermion behaviour, valence fluctuation, large magneto-resistance (MR) effect and large/giant MCE, *etc.* have been observed.^[44-48] Compared to the other transition metals, the research related to Zn, Mg, and Cd-based intermetallic compounds are not too much. This might be a consequence of the difficulty in materials synthesis due to the low boiling point (high vapour pressure) of Zn, Mg, and Cd. Pöttgen et al.^[49, 50] have proposed a simple method to prepare such materials. First, stoichiometric amounts (0.5%~1% of the low boiling point metals were added) of the consistent elementals with purity better than 99.9% were weighted. Second, the weighted metals are arc-welded^[49] in a Ta or Nb tube under an argon pressure of ca. 75-85 kPa. The argon was purified over titanium sponge (900 K), silica gel, and molecular sieves. Third, the crucible was placed in a water-cooled sample chamber of an induction furnace (Hüttinger Elektronik, Freiburg, Germany, Typ TIG 1.5/300)^[50] and heated up to a certain high temperature for several minutes, following by several hours annealing at a selected temperature. Then the obtained samples were grinded and cold-pressed into pellet, and finally annealed at a certain temperature for several days in evacuated quartz tubes. The structural properties and phase purity were subsequently characterized by X-ray powder diffraction (XRD) and Energy Dispersive X-Ray Spectroscopy (EDX) analyses. In the following section, our recent progress related to the magnetism and MCE in the binary or ternary intermetallic compounds of *RE* with

low boiling point metal(s) (Zn, Mg, and Cd) is reviewed, respectively. For a quick comparison, the magnetic transition temperature together with MCE parameters for the compounds in the present review as well as some other rare earth based intermetallic compounds with significant MCE properties are summarized in Table I.

3.1. Zn-based intermetallic compounds

The equiatomic binary compounds $REZn$ (RE is a rare earth) with the cubic CsCl-type structure (space group $Pm\bar{3}m$) have attracted some attention due to their simple crystal structure as well as their interesting physical and chemical properties.^[51-54] The magnetic studies revealed that the heavy $REZn$ compounds order ferromagnetically with the ordering temperature ranging from 267 K for GdZn to 8.5 K for TmZn, whereas the light ones order antiferromagnetically.^[51-54] Sousa et al.^[55, 56] have theoretically investigated the MCE in $REZn$ ($RE = Tb, Ho, \text{ and } Er$), and some anomalies in $\Delta S_M(T)$ curves are found due to spontaneous and/or spin reorientation transitions in these compounds. Very recently, we have experimentally investigated the magnetic phase transition and magnetocaloric properties of $REZn$ ($RE = Tm \text{ and } Ho$) compounds.^[57, 58]

Figure 3 shows the temperature dependence of the zero field cooling (ZFC) and field cooling (FC) magnetization (M) for TmZn under various magnetic fields (H) from 0.1 to 1 T. Both ZFC and FC $M(T)$ curves show a typical PM to FM transition. With increasing magnetic field, T_C increases gradually from 8.4 K for $H = 0.1$ T to 10.3 K for $H = 1$ T. To evaluate the MCE in TmZn, a set of $M(H)$ curves with increasing and decreasing magnetic field up to 7 T together with the temperature dependence of the heat capacity C for TmZn for the magnetic field changes of 0-2 and 0-5 T for TmZn were measured. No obvious hysteresis can be observed for the whole temperature range. Several isotherms with increasing field are presented in Fig. 4 and the corresponding Arrott plot (H/M versus M^2) curves are shown in Fig. 5. For the low temperature ones, the $M(H)$ curves show the typical behavior of a soft ferromagnet. With

increasing temperature higher than 8 K, a field induced metamagnetic transition can be observed in the $M(H)$ curves with a wide temperature range, and resulting in a clear S-shape in the Arrott plots which is a typical characterization for the first-order magnetic phase transition.^[43] Additionally, the observed magnetic properties in TmZn are quite similar to one of the most important class of MCE materials, $RECO_2$ ($RE = Dy, Ho, \text{ and } Er$), which were highlighted due to the occurrence of IEM as well as its close relationship with giant MCE.^[12, 13]

The temperature dependence of $-\Delta S_M$ and ΔT_{ad} for TmZn are shown in Fig. 6 and Fig. 7 which was calculated from the $M(H, T)$ data and from $C(T, H)$, respectively. Both ΔS_M and ΔT_{ad} obtained by using the two methods as described in Section 2 are in good agreement with each other. The values of $-\Delta S_M^{\max}$ are 26.9 and 29.7 J/kg K for the magnetic field changes of 0-5 and 0-7 T, respectively, and the corresponding values of ΔT_{ad} are 8.6 and 11.2 K, indicating that the binary equiatomic compound TmZn belongs to a class of giant magnetocaloric materials. Moreover, for the relatively small field change of 0-1 and 0-2 T, the values of $-\Delta S_M^{\max}$ reach 11.8 and 19.6 J/kg K which is beneficial for application. The observed giant MCE in TmZn is related to the first order, field-induced metamagnetic phase transition. I. e., the field sensitive magnetic transition, sharp changes of magnetization around T_C and large values of magnetization of TmZn are considered to be the origin of the giant MCE. For the magnetic field changes of 0-2, 0-5 and 0-7 T, the values of RCP and RC are determined to be 76, 269 and 422 J/kg, and to be 59, 214 and 335 J/kg, respectively. The corresponding values of ΔT_{ad}^{\max} are estimated to be 3.3, 8.6 and 11.2 K.^[57] These MCE parameters for TmZn (see Table I), especially for the magnetic field change of 0-2 T, are comparable or obviously larger than most of the potential promising magnetic refrigerant materials in the similar temperature region, the applicability of TmZn attractive for low temperature active magnetic refrigeration.^[57]

Whereas, two successive magnetic transitions are observed around $T_C \sim 72$ K and $T_{SR} \sim 26$

K for HoZn which is corresponding to paramagnetic to ferromagnetic and spin reorientation transitions, respectively.^[58] Magnetization and modified Arrott plots indicate that HoZn undergoes a second-order magnetic phase transition around T_C . The critical behaviour around T_C has been performed by modified Arrott plots, scaling analysis and scaling plots and field change dependence on the magnetic entropy change method. The values of critical exponents β , γ and δ for HoZn are determined to be 0.47 ± 0.02 , 1.09 ± 0.03 and 3.32 ± 0.04 , respectively which have some small deviations from the mean-field theory, indicating a short range or a local magnetic interaction which is properly related to the coexistence of FM and SR transitions at low temperature.^[58]

The magnetic entropy change ΔS_M for HoZn was calculated from $M(H, T)$ data (as shown in Fig. 8). One large peak together with a shoulder can be observed in the $-\Delta S_M(T)$ curves around the FM and SR transition temperatures, respectively. Two peaks (shoulder) overlap with each other, resulting in a wide temperature range with a large *RCP* which is beneficial for active applications. The maximum values of the magnetic entropy change ($-\Delta S_M^{\max}$) of HoZn for the magnetic field changes of 0-2, 0-5 and 0-7 T are 6.5, 12.1 and 15.2 J/kg K, respectively. The corresponding values of *RCP* are evaluated to be as large as 255, 792 and 1124 J/kg.^[58] These values are obviously larger than those of recently reported for potential magnetic refrigerant materials with similar working temperature under the same field change (see Table I). The large values of $-\Delta S_M^{\max}$ and *RC* indicate that HoZn could be a promising candidate for active magnetic refrigeration in the temperature range of 30-90 K.^[58]

Hermes et al.^[59] have studied the magnetic properties and MCE in the $\text{EuRh}_{1.2}\text{Zn}_{0.8}$ which crystallizes with the MgCu_2 structure and orders ferromagnetically at $T_C \sim 95$ K. For the magnetic changes of 0-2 and 0-5 T, the values of $-\Delta S_M^{\max}$, $\Delta T_{\text{ad}}^{\max}$ and *RCP* are evaluated to be 3.1 and 5.7 J/kg K, to be 1.4 and 2.8 K, and to be 233 and 513 J/kg, respectively. A large

reversible MCE was reported in EuAuZn around 52 K accompanied by a second order magnetic phase transition from a PM to a FM state.^[60] The values of $-\Delta S_M^{\max}$ for EuAuZn reach 4.8, 9.1 and 11.3 J/kg K for the magnetic field changes of 0-2, 0-5 and 0-7 T, respectively, and show no thermal and magnetic hysteresis around T_C . The corresponding values of $\Delta T_{\text{ad}}^{\max}$ are evaluated to be 2.1, 3.8 and 4.7 K. Very recently, Zhang et al.^[61] have reported the magnetic and magnetocaloric properties in the equiatomic intermetallic compounds of TmZnAl. And they found that the TmZnAl compound undergoes a second order magnetic transition from PM to FM state around 2.8 K. A reversible MCE with considerable magnitude was observed at low temperature. For the magnetic field changes of 0-2, 0-5 and 0-7 T, the maximum values of $-\Delta S_M$ are 4.3, 9.4 and 11.8 J/kg K and the corresponding values RCP (RC) are determined to be 53 (41), 189 (149) and 289 (228) J/kg, respectively, for TmZnAl.

3.2. Mg-based intermetallic compounds

The ternary *RE*-rich intermetallic compounds of the general composition RE_4TMg ($T = \text{Rh, Pd, or Pt}$), crystallizing in the cubic Gd_4RhIn -type structure have attracted some attention due to their interesting physical and chemical properties.^[62-65] For this type of crystal structure, there are three crystallographically independent *RE* sites and the rare structural motif of Mg_4 tetrahedra. The transition metal atoms are located in RE_6 trigonal prisms with strong covalent *RE-T* bonding. These RE_6T basic building units are condensed via common corners and edges to a three-dimensional network in which the cavities are filled by the Mg_4 tetrahedra. Recently, we have reported the magnetic properties and MCE of RE_4PdMg ($RE = \text{Eu and Er}$) and RE_4PtMg ($RE = \text{Ho and Er}$).^[66-68] The magnetic phase transition, the origin of the MCE and its potential application for magnetic refrigeration of these compounds will be shown as below.

Figure 9 (a) shows the temperature dependent ZFC and FC magnetization M (left scale) and dM_{FC}/dT (right scale) under $H = 0.1$ T for Eu_4PdMg . No difference is observed between the

ZFC and FC M - T curves around T_C which is usual in magnetic materials with a second order magnetic transition. Only one peak in dM/dT vs. T is observed around 150 K which is corresponding to the PM to FM magnetic transition. Figure 9 (b) shows the FC magnetization M (left scale) and dM_{FC}/dT (right scale) for Eu_4PdMg under $H = 1$ T. We can note that M increases continuously with decreasing temperature, and dM/dT shows a table-like behaviour from 20 to 150 K.^[66] Fig. 10 shows the $M(T)$ curves for Eu_4PdMg under various magnetic fields up to 7 T. The magnetic transition is very sensitive to the magnetic field, a sharp PM to FM transition can be observed under low magnetic field, and the transition getting broader gradually with increasing magnetic field. The magnetization almost shows linear temperature dependence under higher magnetic fields. This exotic magnetic transition behaviour may be related to its special crystal structure and abundant rare earth site occupation.^[66]

A set of magnetic isotherms were measured for Eu_4PdMg in the temperature range from 3 to 220 K to evaluate its magnetic entropy change. No obvious hysteresis can be observed over the temperature range. Additionally, the order of magnetic phase transition for Eu_4PdMg is confirmed to be second order based on the Banerjee criterion. The resulted $-\Delta S_M(T)$ curves with the magnetic field changes up to 0-7 T is shown in Fig 11. The $-\Delta S_M(T)$ curves show a pronounced peak around T_C for a low magnetic field change which is similar to the typical behaviour for magnetocaloric materials with a single magnetic phase transition.^[66] A very broad table-like behaviour can be observed for a high magnetic field change which is beneficial for application. These peculiar MCE properties in Eu_4PdMg are probably related to the magnetic field sensitive magnetic phase transition and large saturated magnetic moment which is corresponding to its exotic magnetic and/or crystal structure.^[66] With the magnetic field changes of 0-2, 0-5 and 0-7 T, the values of $-\Delta S_M^{\max}$ are 2.6, 5.5 and 7.2 J/kg K, respectively. The corresponding values RCP (RC) are determined to be 53 (41), 189 (149) and 289 (228) J/kg. As

a matter of fact, the values of $-\Delta S_M^{\max}$ are smaller than those of recently reported giant MCE materials at the low temperature region which is related to the additional internal entropy loss due to the larger lattice heat capacity of the materials with the higher T_C . The $-\Delta S_M^{\max}$ value of Eu_4PdMg is comparable with those of some potential magnetic refrigerant materials in the similar temperature region under the same field change (see table I). The RC and RCP values are obviously larger than those of some potential magnetic refrigerant materials at similar temperature region. The excellent MCE properties indicate that Eu_4PdMg is a promising candidate for active magnetic refrigeration in the 20 to 160 K temperature range. The present results may also provide an important clue for searching suitable refrigerant materials in the category of materials that with a field sensitive magnetic phase transition(s).^[66]

Very recently, the magnetic properties and the MCE in Ho_4PtMg , Er_4PdMg , and Er_4PtMg compounds have been investigated by magnetization and heat capacity measurements.^[67-68] The compounds undergo a second order magnetic phase transition from a PM to FM state at Curie temperatures of $T_C \sim 28, 21$ and 16 K for Ho_4PtMg , Er_4PtMg , and Er_4PdMg , respectively. The resulted temperature dependence of $-\Delta S_M$ and ΔT_{ad} with various magnetic field changes up to 0-7 T for Ho_4PtMg , Er_4PdMg and Er_4PtMg are shown in Fig. 12 (a), (b) and (c), and in Fig. 13 (a), (b) and (c), respectively. With the magnetic field changes of 0-1, 0-2, 0-5 and 0-7 T, the values of $-\Delta S_M^{\max}$ are evaluated to be 2.8, 6.1, 13.4 and 16.9 J/kg K, to be 2.8, 6.2, 15.5 and 20.6 J/kg K, and to be 3.9, 8.5, 17.9 and 22.5 J/kg K for Ho_4PtMg , Er_4PdMg and Er_4PtMg , respectively, indicating that the presently studied compounds belong to a class of large MCE materials. For the magnetic field changes of 0-2, 0-5 and 0-7 T, the values of RCP are determined to be 177, 527 and 762 J/kg; 142, 457 and 742 J/kg K; 152, 483 and 716 J/kg K for Ho_4PtMg , Er_4PdMg and Er_4PtMg , and the corresponding values of $\Delta T_{\text{ad}}^{\max}$ are evaluated to be 1.8, 4.1 and 5.3 K, to be 1.7, 3.7 and 5.5 K, and to be 2.2, 5.0 and 6.5 K, respectively. The

values for the presently studied compounds are comparable or even larger than some of the potential promising magnetic refrigerant materials in the similar temperature region, classifying them as considerable candidates for low temperature magnetic refrigeration.^[67, 68]

Linsinger et al.^[69] have studied magnetism and MCE in the $\text{Gd}_2\text{Ni}_x\text{Cu}_{2-x}\text{Mg}$ ($x = 1$ and 0.5) compounds. Both compounds show a large reversible MCE near their ordering temperatures. The values of $-\Delta S_M^{\text{max}}$ reach 9.5 and 11.4 J/kg K for the field change of 0-5 T with no obvious hysteresis loss around 65 K for $x = 0.5$ and $x = 1$, respectively. The corresponding values of RCP reach 688 and 630 J/kg which is relatively high compared to other MCE materials in that temperature range. These results indicate that $\text{Gd}_2\text{Ni}_x\text{Cu}_{2-x}\text{Mg}$ could be a promising system for magnetic refrigeration at temperatures below liquid N_2 . The values of $\Delta T_{\text{ad}}^{\text{max}}$ for $\text{Gd}_2\text{Ni}_{0.5}\text{Cu}_{1.5}\text{Mg}$ reach 1.6 and 3.2 K for the magnetic field changes of 0-2 and 0-5 T, respectively, whereas $\Delta T_{\text{ad}}^{\text{max}}$ for Gd_2NiCuMg is slightly higher with 1.8 K and 4.3 K. Gorsse et al., have investigated the MCE in $\text{Gd}_4\text{Co}_2\text{Mg}_3$ compound.^[70] They found that the compound orders antiferromagnetically below $T_N = 75$ K and shows a field-induced transition at approximately 0.93 T at 6 K. The values of $-\Delta S_M^{\text{max}}$ reach 5.8 and 10.3 J/kg K at 77 K for the magnetic field changes of 0-2 and 0-4.6 T, respectively, which is related to the field-induced magnetic phase transition. The corresponding values of $\Delta T_{\text{ad}}^{\text{max}}$ are 1.3(1) and 3.4(1) K, respectively.

3.3. Cd-based intermetallic compounds

Due to the high toxicity of Cd and its compounds, the Cd-based alloys and compounds have limited technical application, and there is little work on the related topics.^[71-73] Hermes et al.^[72] have investigated the magnetic and MCE properties in Er_4NiCd compound which crystallizes in the Gd_4RhIn type structure. They found that Er_4NiCd shows Curie-Weiss behavior above 50 K with $T_N = 5.9$ K. At field strength of 0.4 T a metamagnetic step is visible,

together with the positive paramagnetic Curie-temperature (7.5 K) indicative for the rather unstable antiferromagnetic ground state. The values of ΔS_M^{\max} reach -7.3 and -18.3 J/kg K, and the resulted *RCP* are 237 and 595 J/kg, for the magnetic field changes of 0-2 and 0-5 T, respectively, for Er_4NiCd . The corresponding values of $\Delta T_{\text{ad}}^{\max}$ are 3.1 and 7.7 K for the magnetic field changes of 0-2 and 0-5 T, respectively. These results indicate that Er_4NiCd could be a promising system for magnetic refrigeration at temperatures below liquid H_2 .^[72]

Recently, Li et al.^[73] have investigated the magnetism and MCE in $\text{GdCd}_{1-x}\text{Ru}_x$ ($x = 0.1, 0.15, \text{ and } 0.2$) solid solutions. Figure 14 shows the temperature dependence of ZFC and FC magnetization for $\text{GdCd}_{1-x}\text{Ru}_x$ under a low magnetic field of $H = 0.1$ T. A typical PM to FM transition can be observed around $T_C \sim 149, 108$ and 73 K for $x = 0.1, 0.15$ and 0.2 , respectively. No obvious thermal hysteresis can be observed between ZFC and FC M - T curves which is benefit for application. To evaluate the MCE in $\text{GdCd}_{1-x}\text{Ru}_x$, a set of $M(H)$ curves around its own T_C were measured. The resulted temperature dependence of $-\Delta S_M$ for $x = 0.1, 0.15$ and 0.2 are shown in Fig. 15 (a), (b) and (c), respectively. The $-\Delta S_M(T)$ curves show pronounced peaks around its own T_C , and the peak is getting sharper and the peak temperature shifts to lower temperature gradually with increasing x . Interestingly, a table-like behaviour in $-\Delta S_M(T)$ curve for $x = 0.1$ can be observed which is benefit for application, especially for a single material. For the magnetic field changes of 0-2, 0-5 and 0-7 T, the values of $-\Delta S_M^{\max}$ are evaluated to be 1.8, 4.1 and 5.6 J/kg K; to be 2.4, 5.8 and 7.8 J/kg K; and to be 3.8, 8.5 and 11.0 J/kg K for $x = 0.1, 0.15$ and 0.2 , respectively.

The $-\Delta S_M^{\max}$ as a function of magnetic field change $\Delta H^{2/3}$ for $\text{GdCd}_{1-x}\text{Ru}_x$ is shown in the inset of Fig. 15 (c). Franco et al.^[74, 75] have previously proposed a universal relation in a magnetic system with second-order phase transition between the $-\Delta S_M^{\max}$ and ΔH , $-\Delta S_M^{\max} \approx A(\Delta H)^n$, where A is a constant. A linear relation between $-\Delta S_M^{\max}$ and $(\Delta H)^{2/3}$ can be observed

for all the present studied samples under high magnetic field changes, indicating the critical behaviour for $\text{GdCd}_{1-x}\text{Ru}_x$ is close to the mean field theory. For the magnetic field change of 0-5 T and 0 to 7 T, the values of RCP for $\text{GdCd}_{1-x}\text{Ru}_x$ are determined 636, 597 and 583 J/kg, and to be 889, 852 and 828 J/kg for $x = 0.1, 0.15$ and 0.2 , respectively. Additionally, the $\text{GdCd}_{1-x}\text{Ru}_x$ solid solutions are quite interesting, since by changing the Ru content, it can cover a wide temperature range with excellent MCE properties and then the materials can be combined to design a composite material used as a magnetic refrigerant. Therefore, the considerable ΔS_M^{\max} without any thermal/magnetic hysteresis and large RCP values together with the tunable T_M indicate that the $\text{GdCd}_{1-x}\text{Ru}_x$ solid solutions are attractive for active magnetic-refrigeration.^[73]

4. Magnetic properties and MCE in $RENi_2B_2C$ superconductors

The quaternary rare earth nickel boroncarbides $RENi_2B_2C$ ($RE =$ rare earth) which crystallize in the tetragonal $\text{LuNi}_2\text{B}_2\text{C}$ -type structure have attracted much attention due to the coexisting of superconductivity and magnetic ordering phenomena.^[99-103] The compounds are long range magnetic ordered for $RE = \text{Gd}, \text{Tb}, \text{Dy}, \text{Ho}, \text{Er},$ and Tm . And the superconductivity is observed for $RE = \text{Y}, \text{Lu}, \text{Dy}, \text{Ho}, \text{Er}$ and Tm . I. e., superconductivity coexists with magnetic order for $RE = \text{Dy}, \text{Ho}, \text{Er},$ and Tm , and the ratio of superconducting transition temperature (T_{SC}) to antiferromagnetic (AF) ordering temperature T_N ranges from $T_{SC} / T_N = 7.0$ for $\text{TmNi}_2\text{B}_2\text{C}$ to 0.60 for $\text{DyNi}_2\text{B}_2\text{C}$ systems.^[101-103] The coexistence and competition of magnetism and superconductivity in these compounds have been systematically investigated experimentally and theoretically.^[99-103] In recent years, we have further investigated the MCE in parent and doped $RENi_2B_2C$ superconductors.^[104-107] The main achievements will be shown in the following sections. The superconducting transition and magnetic ordering temperatures together with MCE parameters are summarized in Table II for a quick comparison of the MCE

in the $RENi_2B_2C$ superconductors.

4.1. Giant reversible MCE in $Dy_{0.9}Tm_{0.1}Ni_2B_2C$ superconductor

Figure 16 shows the low temperature magnetic isothermals on increasing (open symbols) and decreasing (filled symbols) field for $Dy_{0.9}Tm_{0.1}Ni_2B_2C$ at 2 and 3 K as well for $DyNi_2B_2C$ at 2 K for a comparison. A large hysteresis for $DyNi_2B_2C$ was observed, in contrast, the hysteresis of $Dy_{0.9}Tm_{0.1}Ni_2B_2C$ was ignorable for $T \geq 3$ K. The magnetic phase transition T_M and superconducting transition temperature T_{SC} are determined to be 9.2 and 4.5 K, respectively, which are lower than those in $DyNi_2B_2C$.^[102, 104] A set of selected magnetic isothermals $M(H)$ were measured to evaluate the MCE in $Dy_{0.9}Tm_{0.1}Ni_2B_2C$. The $M(H)$ curves were converted to the Arrot-plot of H/M vs. M^2 for $Dy_{0.9}Tm_{0.1}Ni_2B_2C$ at some selected temperatures which reveals the occurrence of a first order magnetic phase transition because there is a clear S-shaped behavior below the transition temperature, based on the Banerjee criterion.^[43]

The resulted magnetic entropy changes $-\Delta S_M$ which was calculated from $M(H, T)$ curves in $Dy_{0.9}Tm_{0.1}Ni_2B_2C$ as a function of temperature are shown in Fig. 17. The temperature and magnetic field change dependences of $-\Delta S_M(T)$ curves provide valuable information on the magnetic ordering in $Dy_{0.9}Tm_{0.1}Ni_2B_2C$. For the magnetic field changes $\Delta H \leq 2$ T, $-\Delta S_M$ is negative (inverse MCE) below the transition temperature, and changes to positive with increasing temperature, which is corresponding to the magnetic transition from PM to AFM state. For $\Delta H \geq 3$ T, a positive $-\Delta S_M$ (i.e. conventional MCE) with a broad peak around 13 K is observed. The values of maximum magnetic entropy change ($-\Delta S_M^{\max}$) reach 14.7 and 19.1 J/kg K for the magnetic field change of 0-5 and 0-7 T, respectively. The giant MCE was believed to be related to the field induced first-order magnetic transition from AFM to FM.^[104] The field dependence of $-\Delta S_M^{\max}$ for $Dy_{0.9}Tm_{0.1}Ni_2B_2C$ is also shown in the inset of Fig 17. The value of $-\Delta S_M^{\max}$ increases continuously with the increasing field, and a faster increase of $-\Delta S_M^{\max}$ with

increasing field was observed above 2 T. I.e. the MCE could attain higher value in higher magnetic fields. The MCE parameters for $\text{Dy}_{0.9}\text{Tm}_{0.1}\text{Ni}_2\text{B}_2\text{C}$ are comparable with those of the potential promising magnetic refrigerant materials in the similar temperature region.^[104]

4.2. Large magnetic entropy change in $\text{Dy}_{1-x}\text{Ho}_x\text{Ni}_2\text{B}_2\text{C}$ ($x = 0 - 1$) superconductors

We have also investigated the superconductivity, magnetic properties and MCE in $\text{Dy}_{1-x}\text{Ho}_x\text{Ni}_2\text{B}_2\text{C}$ ($x = 0 - 1$) superconductors. The superconducting transition temperature T_{SC} and the magnetic ordering temperature T_{M} are determined to be 6.4, 6.4, 6.2, 8.1 and 8.2 K and to be 10, 8.5, 8, 6 and 5 K for $x = 0, 0.3, 0.5, 0.7$ and 1, respectively.^[105, 106] A set of selected magnetic isothermals on increasing and decreasing field for $\text{Dy}_{1-x}\text{Ho}_x\text{Ni}_2\text{B}_2\text{C}$ ($x = 0, 0.3, 0.5, 0.7$ and 1) are measured in the temperature range from 2 to 36 K up to 7 T. Although some hysteresis of $M(H)$ can be observed at low temperatures, it gradually became smaller with increasing temperature, and almost disappeared above 5 K. All the samples show similar behaviors. Several isotherms with increasing field for $x = 0.5$ are presented in Fig. 18(a). To understand the order of magnetic transition in $\text{Dy}_{1-x}\text{Ho}_x\text{Ni}_2\text{B}_2\text{C}$, the measured $M-H$ isotherms were converted in to H/M versus M^2 plots. A clear negative slope at low temperature and low magnetic field region can be observed for all the compounds, the Arrott plots of $x = 0.5$ are shown in Fig. 18(b) for an example, indicating the first order magnetic phase transition for $\text{Dy}_{1-x}\text{Ho}_x\text{Ni}_2\text{B}_2\text{C}$ ($x = 0, 0.3, 0.5, 0.7$ and 1) compounds.^[106]

The magnetic entropy change $-\Delta S_{\text{M}}$ was calculated from magnetization isotherm $M(H, T)$ curves. The resulted temperature dependence of $-\Delta S_{\text{M}}$ is shown in Fig 19 for $x = 0, 0.3, 0.7$ and 1 and Fig. 20 (b) for $x = 0.5$ in $\text{Dy}_{1-x}\text{Ho}_x\text{Ni}_2\text{B}_2\text{C}$. The magnetic entropy change for $\text{Dy}_{0.5}\text{Ho}_{0.5}\text{Ni}_2\text{B}_2\text{C}$ were also calculated from the field and temperature dependence of heat capacity $C(T, H)$ [(as shown in Fig. 20 (a)] using $\Delta S_{\text{M}}(T, \Delta H) = \int_0^T [C(T, H_1) - C(T, H_0)]/T dT$,

and the results are also shown in Fig. 20 (b). The results of entropy changes calculated from $M(T, H)$ and $C(T, H)$ are consistent with each other. For low magnetic field changes, $-\Delta S_M$ is negative (inverse MCE) below the transition temperature, and changes to positive with increasing temperature which can be understood in terms of the FM-AFM phase coexistence and the variation in the ratio of these phases under different magnetic fields. For the magnetic field changes of 0-5 and 0-7 T, a positive $-\Delta S_M$ (i.e. conventional MCE) with a broad peak can be observed. For the magnetic field changes of 0-2, 0-5 and 0-7 T, the maximum values of magnetic entropy change ($-\Delta S_M^{\max}$) are evaluated to be 4.5, 17.1 and 22.1 J/kg K for $x = 0$; to be 7.3, 20.2 and 23.3 J/kg K for $x = 0.3$; to be 5.9, 18.5 and 22.4 J/kg K for $x = 0.5$; to be 6.3, 18.7 and 22.9 J/kg K for $x = 0.7$; and to be 7.3, 19.2 and 22.3 J/kg K for $x = 1$, respectively.^[106] The large magnetic entropy changes in $\text{Dy}_{1-x}\text{Ho}_x\text{Ni}_2\text{B}_2\text{C}$ are believed to be related to the field induced first-order magnetic transition from AFM to FM. The values of RCP are all keeping at same high values in the range of 45-62, 243-290 and 414-510 J/kg for the magnetic field changes of 0-2, 0-5 and 0-7 T, respectively. The values of $-\Delta S_M^{\max}$ and RCP for $\text{Dy}_{1-x}\text{Ho}_x\text{Ni}_2\text{B}_2\text{C}$ ($x = 0, 0.3, 0.5, 0.7$ and 1) are comparable with some of potential magnetic refrigerant materials reported in the same temperature range which indicate that the $\text{Dy}_{1-x}\text{Ho}_x\text{Ni}_2\text{B}_2\text{C}$ compounds could be promising candidates for low temperature magnetic refrigeration.^[106]

4.3. Ni site doping effect on MCE for $\text{RENi}_{2-x}\text{A}_x\text{B}_2\text{C}$ ($RE = \text{Dy}$ and Er)

The magnetic properties and MCE in $\text{DyNi}_{2-x}\text{A}_x\text{B}_2\text{C}$ ($A = \text{Co}$ and Cr , $x = 0.1$, and 0.2) compounds were also investigated. No superconductivity can be observed above 2 K, and the magnetic transition temperature T_M are determined to be 9.8, 8.4, 8.0, 9.2 and 8.8 K for $x = 0$, 0.1 (Co), 0.2 (Co), 0.1 (Cr) and 0.2 (Cr) in $\text{DyNi}_{2-x}\text{A}_x\text{B}_2\text{C}$ system, respectively. Figure 21 shows the magnetic isothermals on increasing (open symbols) and decreasing (filled symbols) field for $\text{DyNi}_{2-x}\text{A}_x\text{B}_2\text{C}$ ($A = \text{Co}$ and Cr , $x = 0.1$ and 0.2) at 2 K, the hysteresis is ignorable for all the

present $\text{DyNi}_{2-x}\text{A}_x\text{B}_2\text{C}$ which is beneficial for application. I. e. similar to that of Dy site Tm substitution, ^[104] Ni site Co or Cr substitution also can effectively reduce (even eliminate) the magnetic hysteresis of $\text{DyNi}_2\text{B}_2\text{C}$.^[107]

To evaluate the MCE in $\text{DyNi}_{2-x}\text{A}_x\text{B}_2\text{C}$ ($A = \text{Co}$ and Cr , $x = 0.1$ and 0.2), a set of magnetic isothermals are measured. All the samples show similar behaviors. Several isotherms of $\text{DyNi}_{1.8}\text{A}_{0.2}\text{B}_2\text{C}$ for $A = \text{Co}$ and Cr are presented in Fig. 22(a) and (b), and the corresponding Arrott-plot are presented in Fig. 22(c) and (d), respectively. Ni site Co or Cr substitution lower the magnetic transition temperature T_M , and reduce the magnetic hysteresis of $\text{DyNi}_2\text{B}_2\text{C}$. The magnetic properties and magnetocaloric effect (MCE) in $\text{DyNi}_{2-x}\text{A}_x\text{B}_2\text{C}$ ($A = \text{Co}$ and Cr , $x = 0.1$, and 0.2) compounds have been studied. Ni site Co or Cr substitution lower the magnetic transition temperature T_M , and reduce the magnetic hysteresis of $\text{DyNi}_2\text{B}_2\text{C}$. A clear negative slope at low temperature and low magnetic field region can be observed in Fig. 22 (c) and (d), indicating the first order magnetic phase transition for $\text{DyNi}_{2-x}\text{A}_x\text{B}_2\text{C}$ ($A = \text{Co}$ and Cr , $x = 0.1$ and 0.2) compounds.

The temperature and field dependences $-\Delta S_M$ for $\text{DyNi}_{2-x}\text{A}_x\text{B}_2\text{C}$ ($A = \text{Co}$ and Cr , $x = 0.1$ and 0.2) were calculated based on the $M(H, T)$ curves (as shown in Fig. 23). For the magnetic field changes of 0-1 and 0-2 T, $-\Delta S_M$ is negative (inverse MCE) below the transition temperature, and changes to positive with increasing temperature, for the magnetic field changes of 0-5 and 0-7 T, a positive $-\Delta S_M$ (i.e., conventional MCE) can be observed. This behaviour is similar to that of $\text{Dy}_{1-x}\text{Ho}_x\text{Ni}_2\text{B}_2\text{C}$ compounds^[106] which can be understood in terms of the FM and AFM phase coexistence and the variation in the ratio of these phases under different magnetic fields. For the magnetic field change of 0-2 T, the minimum and maximum values of $-\Delta S_M$ are evaluated to be -1.4 and 4.7 J/kg K for $\text{DyNi}_{1.9}\text{Co}_{0.1}\text{B}_2\text{C}$, to be -1.9 and 2.3 J/kg K for $\text{DyNi}_{1.8}\text{Co}_{0.2}\text{B}_2\text{C}$, to be -1.4 and 4.9 J/kg K for $\text{DyNi}_{1.9}\text{Cr}_{0.1}\text{B}_2\text{C}$, and to be -0.7 and 4.6 J/kg K for $\text{DyNi}_{1.8}\text{Cr}_{0.2}\text{B}_2\text{C}$,

respectively. The values of $-\Delta S_M^{\max}$ are evaluated to be 16.3, 10.2, 16.1 and 13.7 J/kg K; and to be 19.3, 13.7, 19.1 and 15.8 J/kg K for $x = 0.1$ (Co), 0.2 (Co), 0.1 (Cr) and 0.2 (Cr) in $\text{DyNi}_{2-x}\text{A}_x\text{B}_2\text{C}$ for the magnetic field changes of 0- 5 and 0-7 T, respectively.^[107]

Zhang and Yang^[108] have investigated the magnetic properties and magnetocaloric effect (MCE) in $\text{ErNi}_{2-x}\text{Fe}_x\text{B}_2\text{C}$ ($x = 0, 0.1$ and 0.2) compounds. Similar to those of $\text{DyNi}_{2-x}\text{A}_x\text{B}_2\text{C}$ ($A = \text{Co}$ and Cr , $x = 0.1$ and 0.2), substitution of Fe for Ni lowered the magnetic transition temperature T_M , and reduced the magnetic hysteresis of $\text{ErNi}_2\text{B}_2\text{C}$. The inverse MCE under low magnetic field and at low temperatures is attributed to the nature of antiferromagnetic state for the present $\text{ErNi}_{2-x}\text{Fe}_x\text{B}_2\text{C}$ compounds. A normal MCE was observed under higher magnetic field changes, which is related to a field-induced first order metamagnetic transition from AFM to FM state. The maximum values of magnetic entropy change $-\Delta S_M^{\max}$ are 14.5, 12.7 and 10.6 J/kg K for the magnetic field change of 0-7 T for $x = 0, 0.1$ and 0.2 in $\text{ErNi}_{2-x}\text{Fe}_x\text{B}_2\text{C}$, respectively.^[108]

5. Summary

Investigations on MCE are of great interest for fundamental properties and technological application. Our recent progress of the magnetic properties and MCE as well as its origin and potential application for magnetic refrigeration in some rare earth based intermetallic compounds are reviewed, and some of them are possess excellent MCE properties. The main achievements are: 1) The TmZn compound exhibits a ferromagnetic state below the Curie temperature of $T_C = 8.4$ K, and processes a field-induced metamagnetic phase transition around and above T_C , resulting in a giant reversible MCE. Particularly, the values of $-\Delta S_M^{\max}$ reach 11.8 and 19.6 J/kg K for a low magnetic field changes of 0-1 and 0-2 T, respectively, indicating that TmZn could be a promising candidate for low temperature and low field magnetic refrigeration. 2) A single phased Eu_4PdMg compounds was synthesised by induction melting of the elements

in a sealed tantalum tube in a water-cooled sample chamber. Eu_4PdMg has a very magnetic field sensitive magnetic phase transition, resulting in a reversible, table-like MCE over a broad temperature range. Additionally, the RCP values are obviously larger than those of some potential magnetic refrigerant materials at similar temperature region, making Eu_4PdMg attractive for magnetic refrigeration from 20 to 160 K. 3) The $\text{GdCd}_{1-x}\text{Ru}_x$ solid solutions with $x = 0.1, 0.15$ and 0.2 have been successfully synthesized and the magnetism and MCE have been investigated. The samples undergo a second order magnetic phase transition from a paramagnetic to a ferromagnetic state at Curie temperatures of $T_C \sim 160, 108$ and 73 K for $x = 0.1, 0.15$ and 0.2 , respectively. A large reversible MCE with a wide temperature range in $\text{GdCd}_{1-x}\text{Ru}_x$ solid solutions was observed which make the $\text{GdCd}_{1-x}\text{Ru}_x$ solid solutions considerable for active magnetic-refrigeration. 4) The Tm substitution effectively reduces the thermal hysteresis of $\text{DyNi}_2\text{B}_2\text{C}$, therefore, a giant reversible MCE has been observed in antiferromagnetic superconductor $\text{Dy}_{0.9}\text{Tm}_{0.1}\text{Ni}_2\text{B}_2\text{C}$ which is related to a field-induced first order metamagnetic transition from AFM to FM state. 5) The magnetic transition temperature T_M as well as the temperature of $-\Delta S_M^{\max}$ in antiferromagnetic superconductors $\text{Dy}_{1-x}\text{Ho}_x\text{Ni}_2\text{B}_2\text{C}$ gradually shifts to low temperature with increasing x , while the values of $-\Delta S_M^{\max}$ remain at almost the same high value which make the $\text{Dy}_{1-x}\text{Ho}_x\text{Ni}_2\text{B}_2\text{C}$ compounds attractive for active magnetic-refrigeration for low temperature magnetic refrigeration. The present results may provide some valuable information for searching proper magnetic materials for low temperature magnetic refrigeration.

References

- [1] Warburg E 1881 *Ann. Phys. (Leipzig)* **13** 141
- [2] Debye P 1926 *Ann. Phys.* **81** 1154
- [3] Giauque W F 1927 *J. Am. Chem. Soc.* **49** 1864
- [4] Giauque W F and MacDougall D P 1933 *Phys. Rev.* **43** 768

- [5] Li R, Numazawa T, Hashimoto T, Tomoyiko A, Goto T and Todo S 1986 *Adv. Cryog. Eng.* **32** 287
- [6] McMichael R D, Ritter J J and Shull R D J 1993 *Appl. Phys.* **73** 6946
- [7] Pecharsky V K and Gschneidner K A Jr 1999 *J. Magn. Magn. Mater.* **200** 44
- [8] Tishin A M 1999 *Handbook of Magnetic Materials* (North-Holland: Amsterdam) **12** 395
- [9] Zimm C, Jastrab A, Sternberg A, Pecharsky V K, Gschneidner K Jr, Osborne M and Anderson I 1998 *Adv. Cryog. Eng.* **43** 1759
- [10] Pecharsky V K and Gschneidner K A Jr 1997 *Phys. Rev. Lett.* **78** 4494
- [11] Gschneidner K A Jr, Pecharsky V K and Tsoko A O 2005 *Rep. Prog. Phys.* **68** 1479 and references therein
- [12] Singh N K, Suresh K G, Nigam A K, Malik S K, Coelho A A and Gama S 2007 *J. Magn. Magn. Mater.* **317** 68
- [13] Gratz Z and Markosyan A S 2001 *J. Phys.: Condens. Matter* **3** R385
- [14] Bruck E 2005 *J. Phys. D: Appl. Phys.* **38** R381
- [15] Tegus O, Bruck E, Buschow K H J and De Boer F R 2002 *Nature* (London) **415** 150
- [16] Wada H and Tanabe Y 2001 *Appl. Phys. Lett.* **79** 3302
- [17] Yue M, Zhang H G, Liu D M and Zhang J X 2015 *Chin. Phys. B* **24** 017505
- [18] Zhong W, Au C K and Du Y W 2013 *Chin. Phys. B* **22** 057501
- [19] Phan M H and Yu S C 2007 *J. Magn. Magn. Mater.* **308** 325 and references therein
- [20] Liu J, Gottschall T, Skokov K P, Moore J D and Gutfleisch O 2012 *Nature Mater.* **11** 620
- [21] Li Z, Xu K, Zhang Y, Tao C, Zheng D and Jing C 2015 *Sci. Rep.* **5** 15413
- [22] Liu J 2014 *Chin. Phys. B* **23** 047503
- [23] Hu F X, Shen B G and Sun J R 2013 *Chin. Phys. B* **22** 037505
- [24] Hu F X, Shen B G, Sun J R, Cheng Z H, Rao G H and Zhang X X 2001 *Appl. Phys. Lett.* **78** 3675
- [25] Hu F X, Shen B G, Sun J R, Wang G J and Cheng Z H 2002 *Appl. Phys. Lett.* **80** 826
- [26] Shen B G, Sun J R, Hu F X, Zhang H W and Cheng Z H 2009 *Adv. Mater.* **21** 4545 and references therein
- [27] Shen B G, Hu F X, Dong Q Y and Sun J R 2013 *Chin. Phys. B* **22** 017502
- [28] Fujita A, Fujieda S, Hasegawa Y and Fukamichi K 2003 *Phys. Rev. B* **67** 104416
- [29] Zhang C L, Shi H F, Ye E J, Nie Y G, Han Z D, Qian B and Wang D H 2015 *Appl. Phys. Lett.* **107** 212403
- [30] Liu E K, Wang W H, Feng L, Zhu W, Li G J, Chen J L, Zhang H W, Wu G H, Jiang C B,

- Xu H B and Boer de F R 2012 *Nat. Commun.* **3** 873
- [31] Wei Z Y, Liu E K, Li Y, Xu G Z, Zhang X M, Liu G D, Xi X K, Zhang H. W, Wang H, Wu G H and Zhang X X 2015 *Adv. Electron. Mater.* **11500076**
- [32] Wang D H, Han Z D, Xuan H C, Ma S C, Chen S Y, Zhang C L and Du Y W 2013 *Chin. Phys. B* **22** 077506 and references therein
- [33] Zhang H and Shen B G *Chin. Phys. B* in press and references therein
- [34] Franco V, Blazquez J S, Ingale B and A. Conde 2012 *Ann. Rev. Mater. Res.* **42** 305 and references therein
- [35] Manosa L, Planes A and Acet M 2013 *J. Mater. Chem. A.* **1** 4925 and references therein
- [36] Li L W, Namiki T, Huo D, Qian Z and Nishimura K 2013 *Appl. Phys. Lett.* **103** 222405
- [37] Gschneidner K A Jr and Pecharsky V K 2000 *Annu. Rev. Mater. Sci.* **30** 387 and references therein
- [38] Kitanovski A and Egolf P W 2010 *Int. J. Refrig.* **38** 449
- [39] Oliveira de N A and Ranke von P J 2010 *Phys. Rep.* **489** 89
- [40] Gutfleisch O, Willard M A, E Bruck, Chen C H, Sankar S G and Liu J Ping 2011 *Adv. Mater.* **23** 821
- [41] Inoue J and Shimizu M 1982 *J. Phys. F: Met. Phys.* **12** 1811
- [42] Liu X B and Altounian Z 2005 *J. Magn. Magn. Mater.* **292** 83
- [43] Banerjee B K 1964 *Phys. Lett.* **12** 16
- [44] Taylor K N R 1971 *Adv. Phys.* **20** 551
- [45] Buschow K H J 1977 *Rep. Prog. Phys.* **40** 1179
- [46] Adroja D T and Malik S K. 1991 *J. Magn. Magn. Mater.* **100** 126
- [47] Kalychak Ya M, Zaremba V I, Pöttgen R, Lukachuk M and Hoffmann R-D 2004 *Handbook on the Physics and Chemistry of Rare Earths* **34** 1
- [48] Gupta S and Suresh K G 2015 *J. Alloys Compd.* **618** 562
- [49] Pöttgen R, Gulden Th and Simon A 1999 *GIT Labor-Fachzeitschrift* **43** 133
- [50] Pöttgen R, Lang A, Hoffman R-D, Künnen B, Kotzyba G, Müllmann R, Mosel B D and Rosenhahn C 1999 *Z Kristallogr.* **214** 143
- [51] Morin P, Rouchy J and Lacheisserie E T 1977 *Phys. Rev. B* **16** 3182
- [52] Galéra R M, Joly Y, Rogalev A and Binggeli N 2008 *J. Phys.: Condens. Matter* **20** 395217
- [53] Jeromen A and Trontelj Z 2005 *J. Appl. Phys.* **98** 033515
- [54] Givord D, Morin P and Schmitt D 1982 *J. Appl. Phys.* **53** 2445
- [55] Sousa de V S R, Plaza E J R and Ranke von P J 2010 *J. Appl. Phys.* **107** 103928

- [56] Sousa de V S R, Ranke von P J and Gandra F C G 2011 *J. Appl. Phys.* **109** 063904
- [57] Li L W, Yuan Y, Zhang Y, Namiki T, Nishimura K, Pöttgen R and Zhou S 2015 *Appl. Phys. Lett.* **107** 132401
- [58] Li L W, Yuan Y, Zhang Y, Pöttgen R and Zhou S 2015 *J. Alloys Compd.* **643** 147
- [59] Hermes W, Harmening T and Pöttgen R 2009 *Chem. Mater.* **21** 3325
- [60] Li L W, Niehaus O, Gerke B and Pöttgen R 2014 *IEEE Trans. Magn.* **50** 2503604
- [61] Zhang Y K, Hou L, Ren Z M, Li X, Wilde G 2016 *J. Alloys Compd.* **565** 635
- [62] Kersting M, Matar S F, Schwickert C and Pöttgen R 2012 *Z. Naturforsch.* **67b** 61
- [63] Couillaud Y S, Linsinger S, Duée C, Rougier A, Chevalier B, Pöttgen R and Bobet J -L 2010 *Intermetallics* **18** 1115
- [64] Tappe F, Scheickert C, Linsinger S and Pöttgen R 2011 *Monatsh. Chem.* **142** 1087
- [65] Mater S F, Chevalier B B and Pöttgen R 2012 *Intermetallics* **31** 88
- [66] Li L W, Niehaus O, Kersting M and Pöttgen R 2014 *Appl. Phys. Lett.* **104** 092416
- [67] Li L W, Niehaus O, Kersting M and Pöttgen R 2015 *Intermetallics* **62** 17
- [68] Li L W, Niehaus O, Kersting M and Pöttgen R 2015 *IEEE Trans. Magn.* **51** 2503804
- [69] Linsinger S, Hermes W, Eul M and Pöttgen R 2010 *J. Appl. Phys.* **108** 043903
- [70] Gorsse S, Chevalier B, Tuncel S and Pöttgen R 2009 *J. Solid State Chem.* **182** 948
- [71] Tappe F and Pöttgen R 2011 *Rev. Inorg. Chem.* **31** 5 and references therein
- [72] Hermes W, Rodewals U C and Pöttgen R 2010 *J. Appl. Phys.* **108** 113919
- [73] Li L W, Niehaus O, Johnscher M and Pöttgen R 2015 *Intermetallics* **60** 9
- [74] Franco V, Blázquez J S and Conde A 2006 *Appl. Phys. Lett.* **89** 222512
- [75] Franco V, Conde A, Romero-Enrique J M and Blázquez J S 2008 *J. Phys.: Condens. Matter* **20** 285207
- [76] Li L W, Hutchison W D, Huo D, Namiki T, Qian Z and Nishimura K 2012 *Scripta Mater.* **67** 237
- [77] Li L W, Hu G, Umehara I, Huo D, Hutchison W D, Namiki T and Nishimura K 2013 *J. Alloys Compd.* **575** 1
- [78] Li L W, Kadonaga M, Huo D, Qian Z, Namiki T and Nishimura K 2012 *Appl. Phys. Lett.* **101** 122401
- [79] Zhang Y K and Wilde G 2015 *Physica B* **472** 56
- [80] Li L W, Saensunon B, Hutchison W D, Huo D and Nishimura K 2014 *J. Alloys Compd.* **582** 670
- [81] Li L W, Nishimura K, Hutchison W D, Qian Z, Huo D and Namiki T 2012 *Appl. Phys. Lett.*

- [82] Mo Z J, Shen J, Yan L Q, Wu J F, Tang C C and Shen B G 2013 *J. Alloys Compd.* **572** 1
- [83] Li L W, Nishimura K, Usui G, Huo D and Qian Z 2012 *Intermetallics* **23** 101
- [84] Zhang Y K, Yang B J and Wilde G 2015 *J. Alloys Compd.* **619** 12
- [85] Zhang Y K and Wilde G 2015 *IEEE Trans. Magn.* **51** 2503104
- [86] Li L W, Igawa H, Nishimura K and Huo D 2011 *J. Appl. Phys.* **109** 083901
- [87] Li L W, Namiki T, Huo D, Qian Z and Nishimura K 2013 *Appl. Phys. Lett.* **103** 222405
- [88] Li L W, Nishimura K and Yamane H 2009 *Appl. Phys. Lett.* **94** 102509
- [89] Li L W, Huo D, Igawa H and Nishimura K 2011 *J. Alloys Compd.* **509** 1796
- [90] Wang J L, Campbell S J, Cadogan J M, Studer A, Zeng R and Dou S X 2011 *Appl. Phys. Lett.* **98** 232509
- [91] Li L W, Nishimura K, Igawa H and Huo D 2011 *J. Alloys Compd.* **509** 4198
- [92] Zhang Y K, Wilde G, Li X, Ren Z M and Li L W 2015 *Intermetallics* **65** 61
- [93] Zhang H, Sun Y J, Niu E, Yang L H, Shen J, Hu F X, Sun J R and Shen B G 2013 *Appl. Phys. Lett.* **103** 202412
- [94] Zhang Q, Cho J H, Li B, Hu W J, Zhang Z D 2009 *Appl. Phys. Lett.* **94** 182501
- [95] Bingham N S, Wang H, Qin F, Peng H X, Sun J F, Franco V, Srikanth H and Phan M H 2012 *Appl. Phys. Lett.* **101** 102407
- [96] Xia L, Tang M B, Chan K C, Dong Y D 2014 *J. Appl. Phys.* **115** 223904
- [97] Li L W, Huo D, Qian Z and Nishimura K 2014 *Intermetallics* **46** 231
- [98] Schäfer K, Schwickert C, Niehaus O, Winter F and Pöttgen R 2014 *Solid. State Sci.* **35** 66
- [99] Cava R J, Takagi H, Zandbergen H W, Krajewski J J, Peck W F, Siegrist T Jr, Batlogg B, Dover van R B, Felder R J, Mizuhashi K, Lee J O, Eisaki H and Uchida S 1994 *Nature (London)* **367** 252
- [100] Canfield P C, Gammel P L and Bishop D J 1998 *Phys. Today* **41** 40
- [101] Muller K H and Narozhnyi V N 2001 *Rep. Prog. Phys.* **64** 943
- [102] Li L W, Nishimura K, Fujii M, Matsuda K and Huo D 2010 *Phys. Rev. B* **81** 214517
- [103] Wolowiec C T, White B D and Maple M B 2015 *Physica C* **514** 113
- [104] Li L W and Nishimura K 2009 *Appl. Phys. Lett.* **95** 132505
- [105] Li L W, Nishimura K, Huo D, Kadonaga M, Namiki T and Qian Z 2011 *Appl. Phys. Express* **4** 093101
- [106] Li L W, Nishimura K, Kadonaga M, Qian Z and Huo D 2011 *J. Appl. Phys.* **110** 043912
- [107] Li L W, Fan H, Matsui S, Huo D and Nishimura K 2012 *J. Alloys Compd.* **529** 25

Figure captions

Fig. 1. (Colour online) The total entropy S as function of magnetic field H and temperature T schematically illustrating the definition of the isothermal magnetic entropy change ΔS_M and the adiabatic temperature change ΔT_{ad} .

Fig. 2. (Colour online) An example for the definition of the relative cooling power (RCP) and refrigerant capacity (RC) for $GdRu_{0.2}Cd_{0.8}$. Rectangular area is RCP and the area full with parallel lines is RC .

Fig. 3. Temperature dependence of the zero field cooling (ZFC) and field cooling (FC) magnetization (M) for TmZn under various magnetic fields (H) up to 1 T. ^[57]

Fig. 4. Magnetic field dependence of the magnetization (increasing field only) for TmZn at some selected temperatures. ^[57]

Fig. 5. The plots of H/M versus M^2 for TmZn at some selected temperatures. ^[57]

Fig. 6. (Colour online) Temperature dependence of magnetic entropy change $-\Delta S_M$ for TmZn with the magnetic field changes up to 0-7 T. ^[57]

Fig. 7. (Colour online) Temperature dependence of adiabatic temperature change ΔT_{ad} for TmZn compound with the magnetic field changes up to 0-7 T. ^[57]

Fig. 8. The magnetic entropy change $-\Delta S_M$ as a function of temperature for various magnetic field changes up to 0-7 T for HoZn. ^[58]

Fig. 9. (Colour online) (a): Temperature dependence of zero field cooling (ZFC) and field cooling (FC) magnetization M (left scale) as well as dM_{FC}/dT (right scale) for Eu_4PdMg in an external magnetic field $H = 0.1$ T. (b): Temperature dependence of FC magnetization M (left scale) and dM_{FC}/dT (right scale) for Eu_4PdMg under $H = 1$ T. ^[66]

Fig. 10. Temperature dependences of the magnetization for Eu_4PdMg under various magnetic fields up to 7 T. ^[66]

Fig. 11. Temperature dependence of magnetic entropy change $-\Delta S_M$ for Eu_4PdMg with the magnetic field changes up to 0-7 T. ^[66]

Fig. 12. Temperature dependence of magnetic entropy change $-\Delta S_M$ with the magnetic field

- changes up to 0-7 T for Ho₄PtMg (a), Er₄PdMg (b) and Er₄PtMg (c), respectively. [67, 68]
- Fig. 13. Temperature dependence of adiabatic temperature change ΔT_{ad} with the magnetic field changes up to 0-7 T for Ho₄PtMg (a), Er₄PdMg (b) and Er₄PtMg (c), respectively. [67, 68]
- Fig. 14. (Colour online) Temperature dependence of zero field cooling (ZFC) and field cooling (FC) magnetization M for GdCd_{1-x}Ru_x ($x = 0.1, 0.15, \text{ and } 0.2$) under a low magnetic field of $H = 0.1$ T. [73]
- Fig. 15. Temperature dependence of magnetic entropy change $-\Delta S_{\text{M}}$ with various magnetic field changes for GdCd_{1-x}Ru_x ($x = 0.1, 0.15, \text{ and } 0.2$). The inset of (c) shows the maximum magnetic entropy change $-\Delta S_{\text{M}}^{\text{max}}$ as a function of magnetic field change $\Delta H^{2/3}$. [73]
- Fig. 16. Magnetic isothermals on increasing (open symbols) and decreasing (filled symbols) field for Dy_{0.9}Tm_{0.1}Ni₂B₂C at 2 and 3 K as well for DyNi₂B₂C at 2 K. [104]
- Fig. 17. Temperature dependence of magnetic entropy change $-\Delta S_{\text{M}}$ for Dy_{0.9}Tm_{0.1}Ni₂B₂C. The inset shows the maximum values of magnetic entropy change $-\Delta S_{\text{M}}^{\text{max}}$ as a function of magnetic field changes. [104]
- Fig. 18. (a) Magnetic field dependence of the magnetization for Dy_{0.5}Ho_{0.5}Ni₂B₂C at some selected temperatures. (b): The plots of H/M versus M^2 for Dy_{0.5}Ho_{0.5}Ni₂B₂C at some selected temperatures. [105]
- Fig. 19. Temperature dependence of magnetic entropy change $-\Delta S_{\text{M}}$ calculated from $M(T, H)$ for Dy_{1-x}Ho_xNi₂B₂C ($x = 0, 0.3, 0.7 \text{ and } 1$). [105]
- Fig. 20. (Colour online) (a) Temperature dependence of heat capacity under the magnetic field of 0 T, 2 T and 5 T for Dy_{0.5}Ho_{0.5}Ni₂B₂C. (b) Temperature dependence of magnetic entropy change $-\Delta S_{\text{M}}$ for Dy_{0.5}Ho_{0.5}Ni₂B₂C calculated from $C(T, H)$ and $M(T, H)$, respectively. [105]
- Fig. 21. (Colour online) Magnetic isothermals on increasing (open symbols) and decreasing (filled symbols) field at 2 K for DyNi_{2-x}A_xB₂C ($A = \text{Co and Cr}, x = 0.1 \text{ and } 0.2$). [107]
- Fig. 22. Magnetic isothermals at some selected temperature for DyNi_{1.8}Co_{0.2}B₂C (a) and DyNi_{1.8}Cr_{0.2}B₂C (b). The curves of H/M versus M^2 for DyNi_{1.8}Co_{0.2}B₂C (c) and DyNi_{1.8}Cr_{0.2}B₂C (d) at some selected temperatures. [107]
- Fig. 23. Temperature dependence of magnetic entropy change $-\Delta S_{\text{M}}$ for DyNi_{2-x}A_xB₂C ($A = \text{Co and Cr}, x = 0.1 \text{ and } 0.2$). [107]

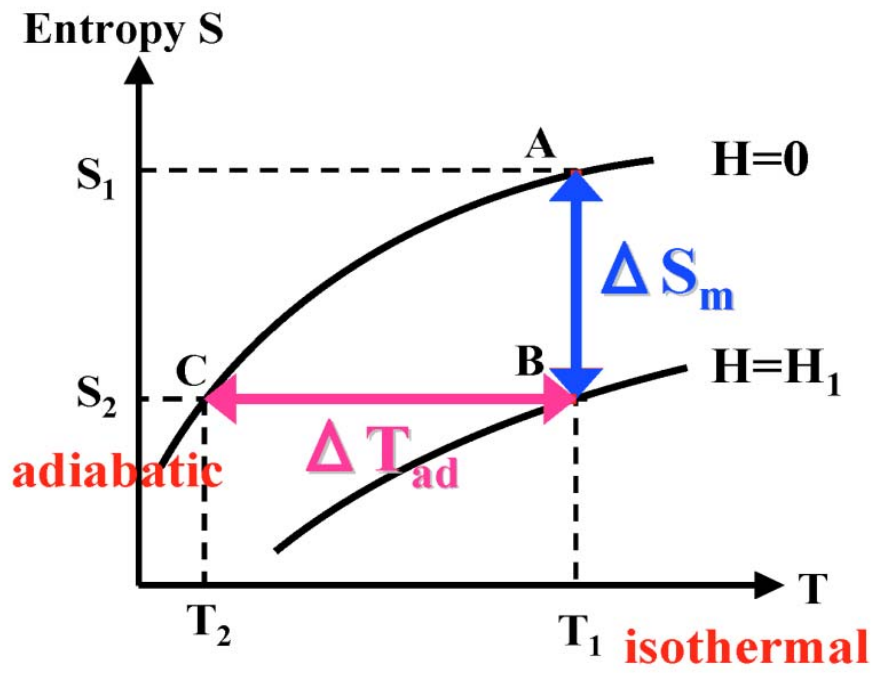


Fig. 1.

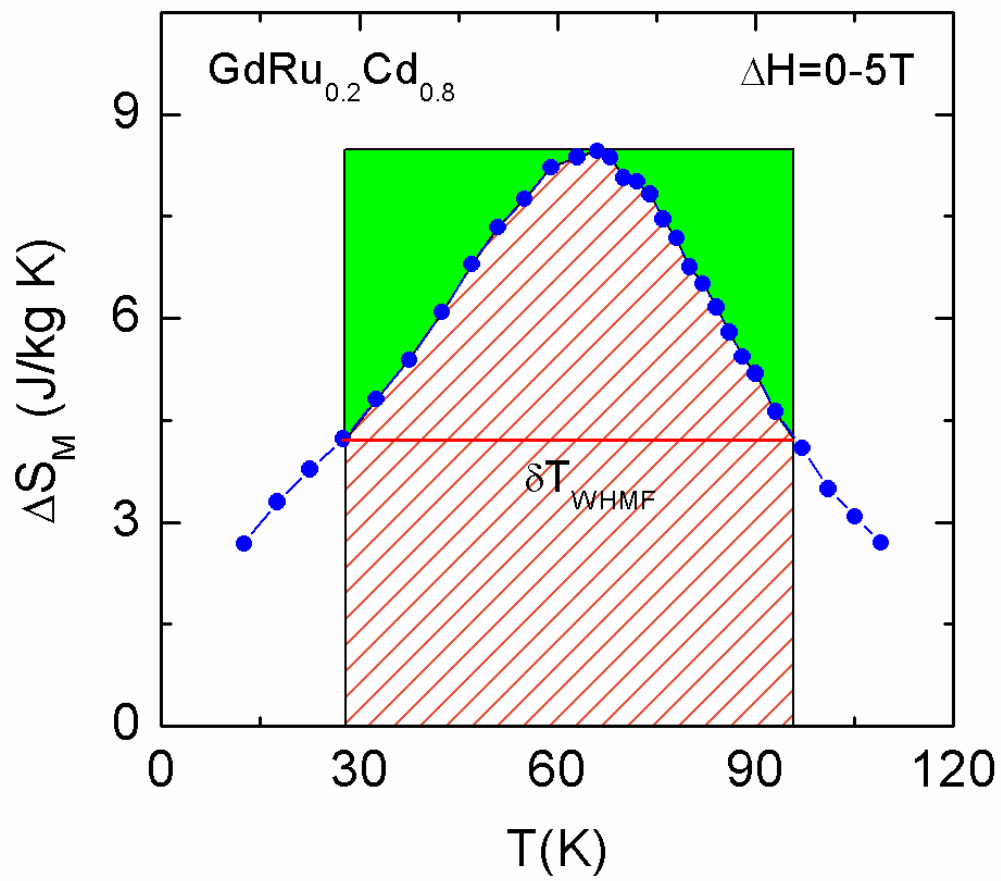


Fig. 2.

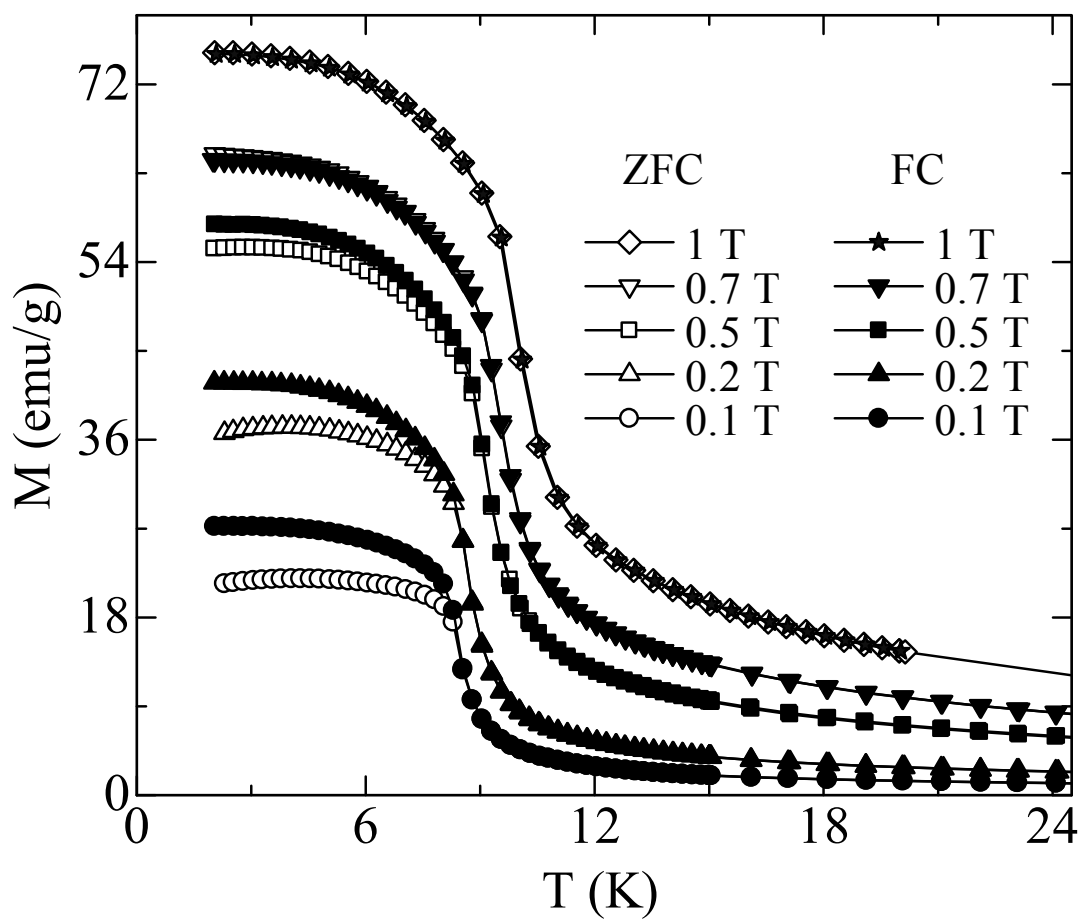


Fig. 3.

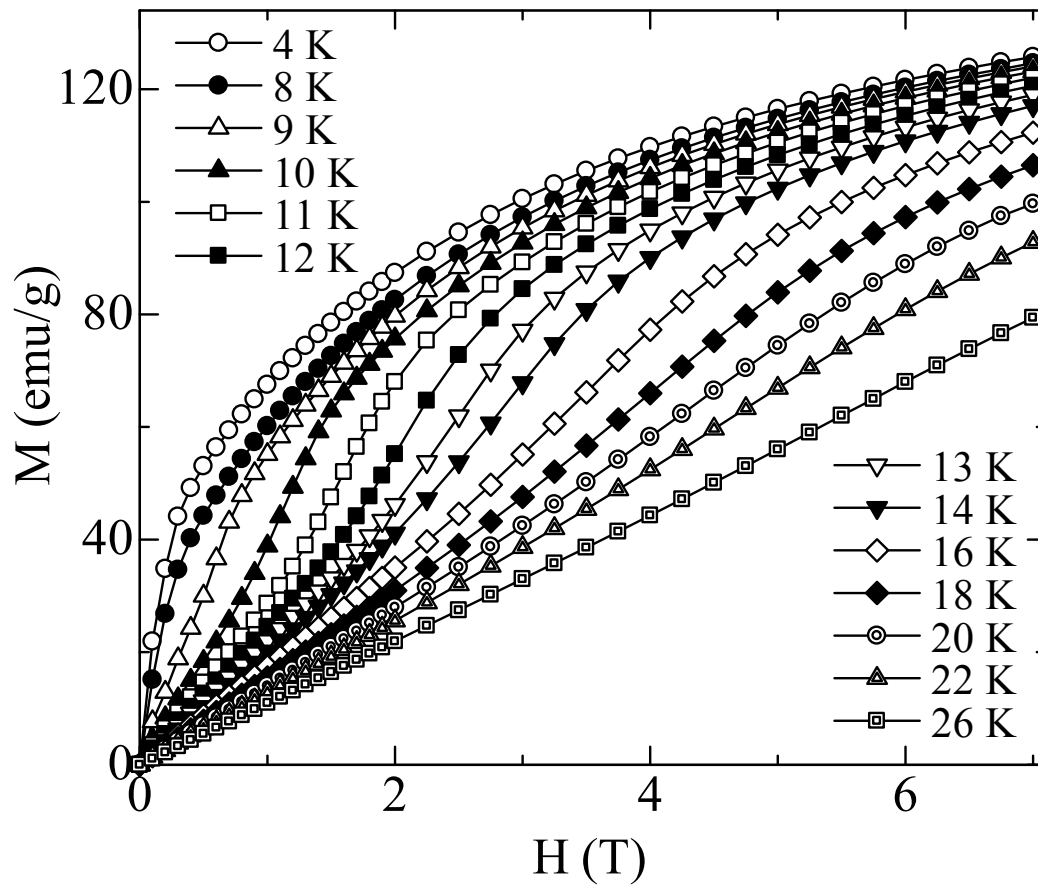


Fig. 4.

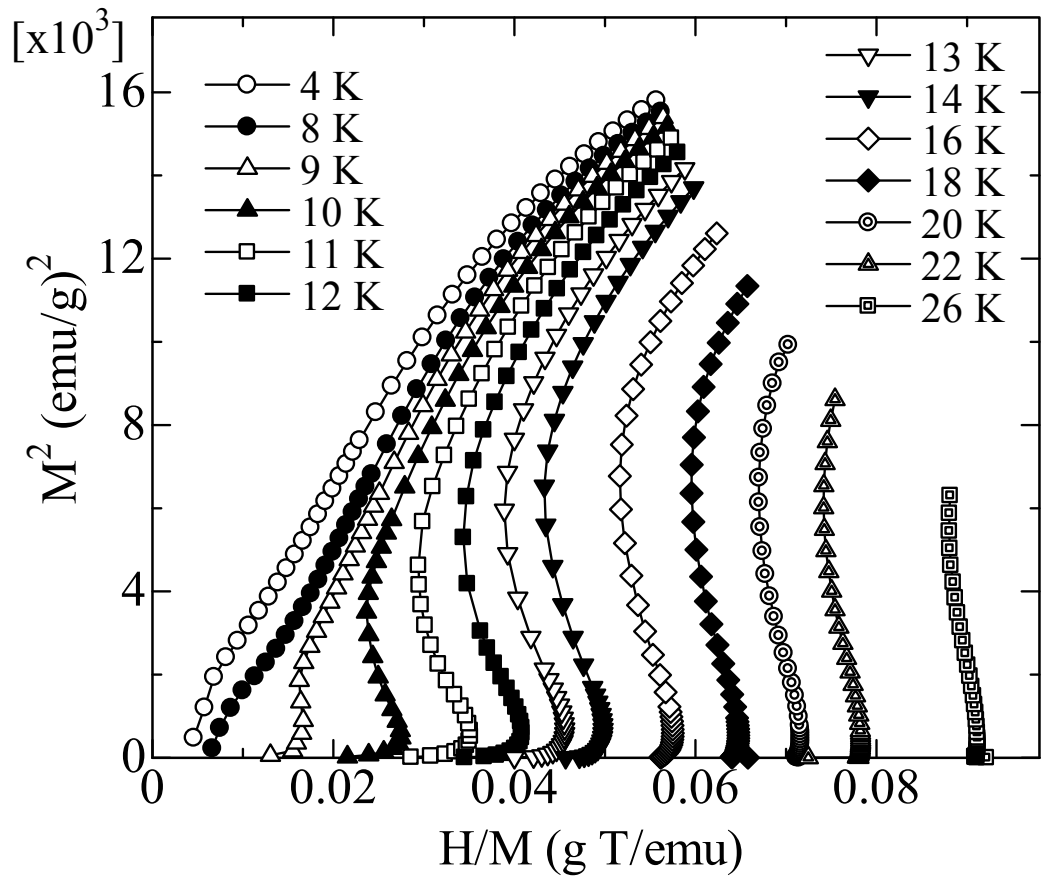


Fig. 5.

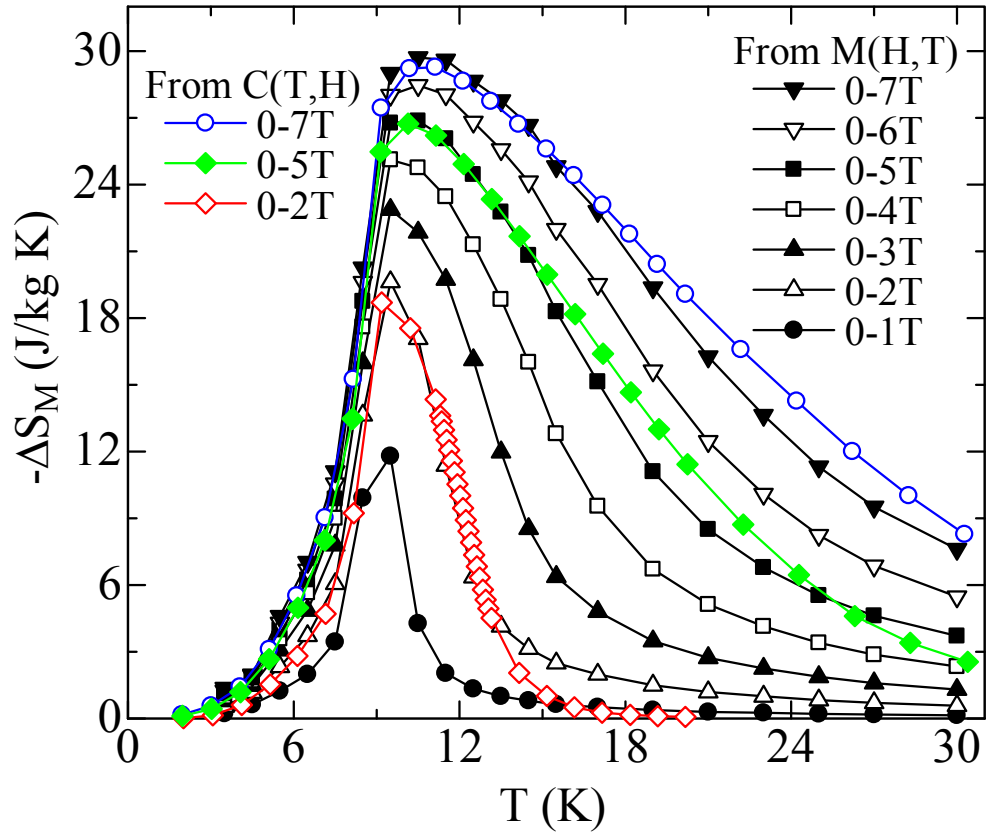


Fig. 6.

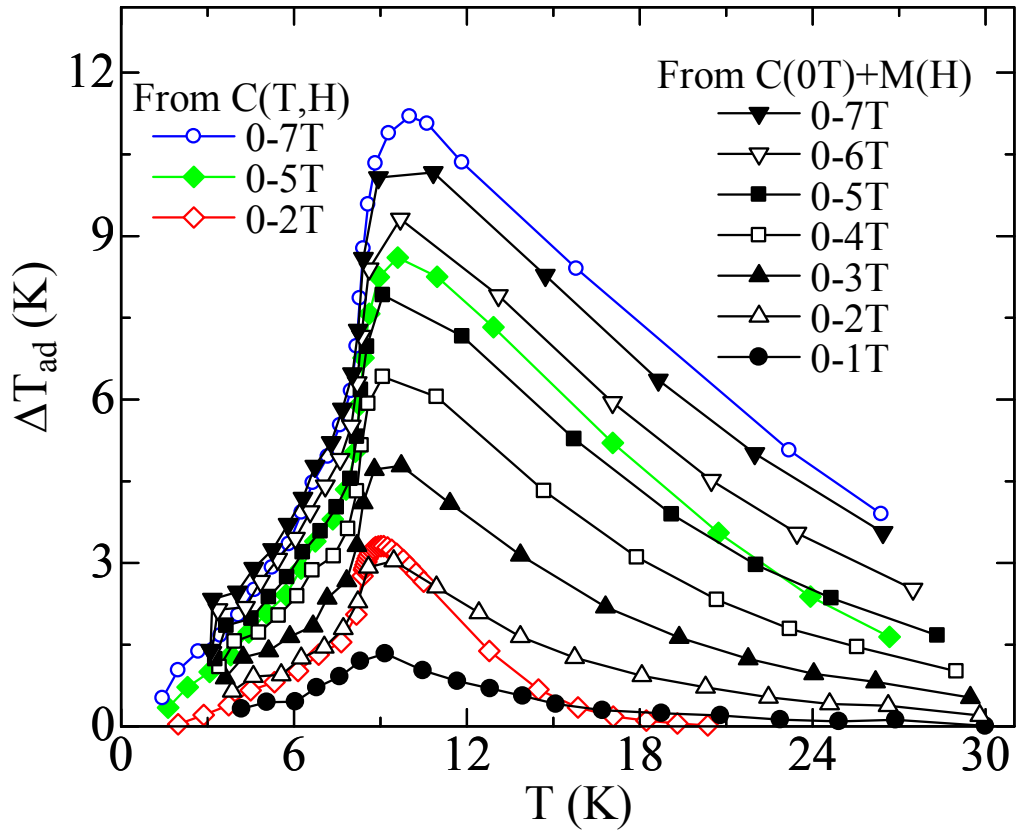


Fig. 7.

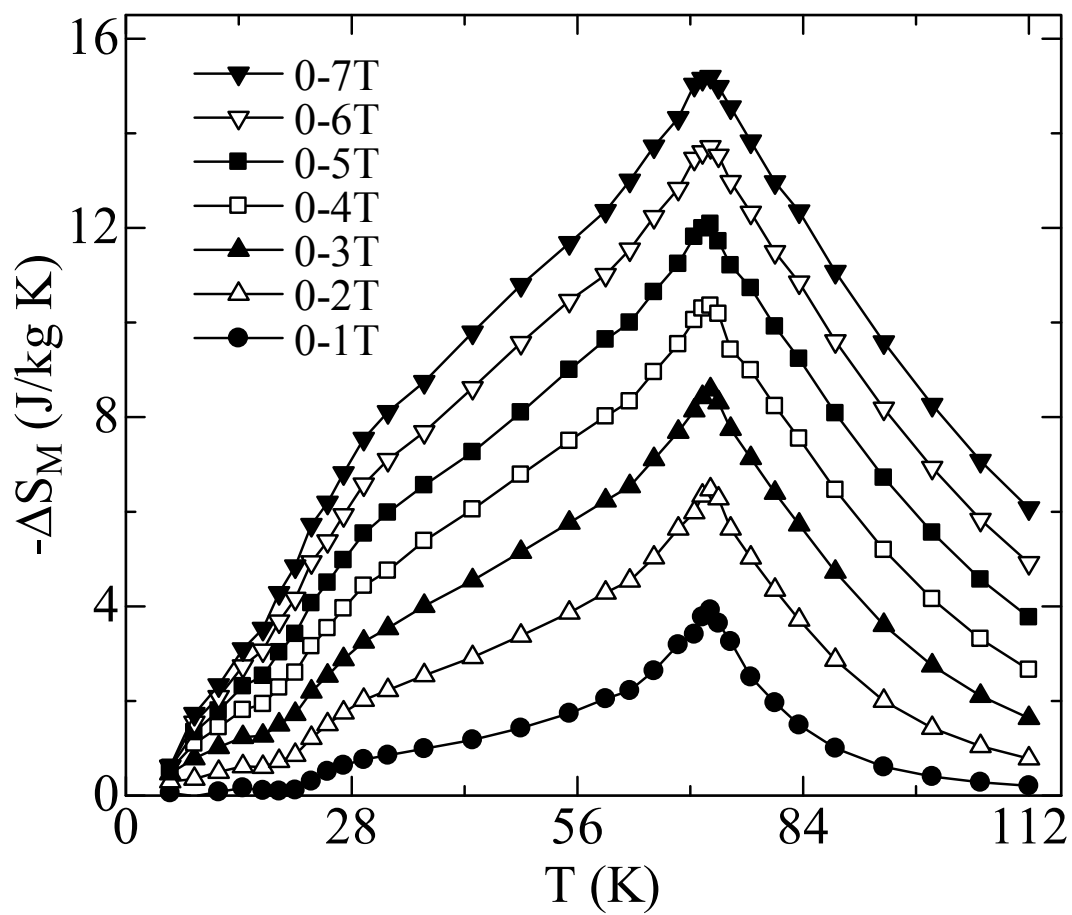


Fig. 8.

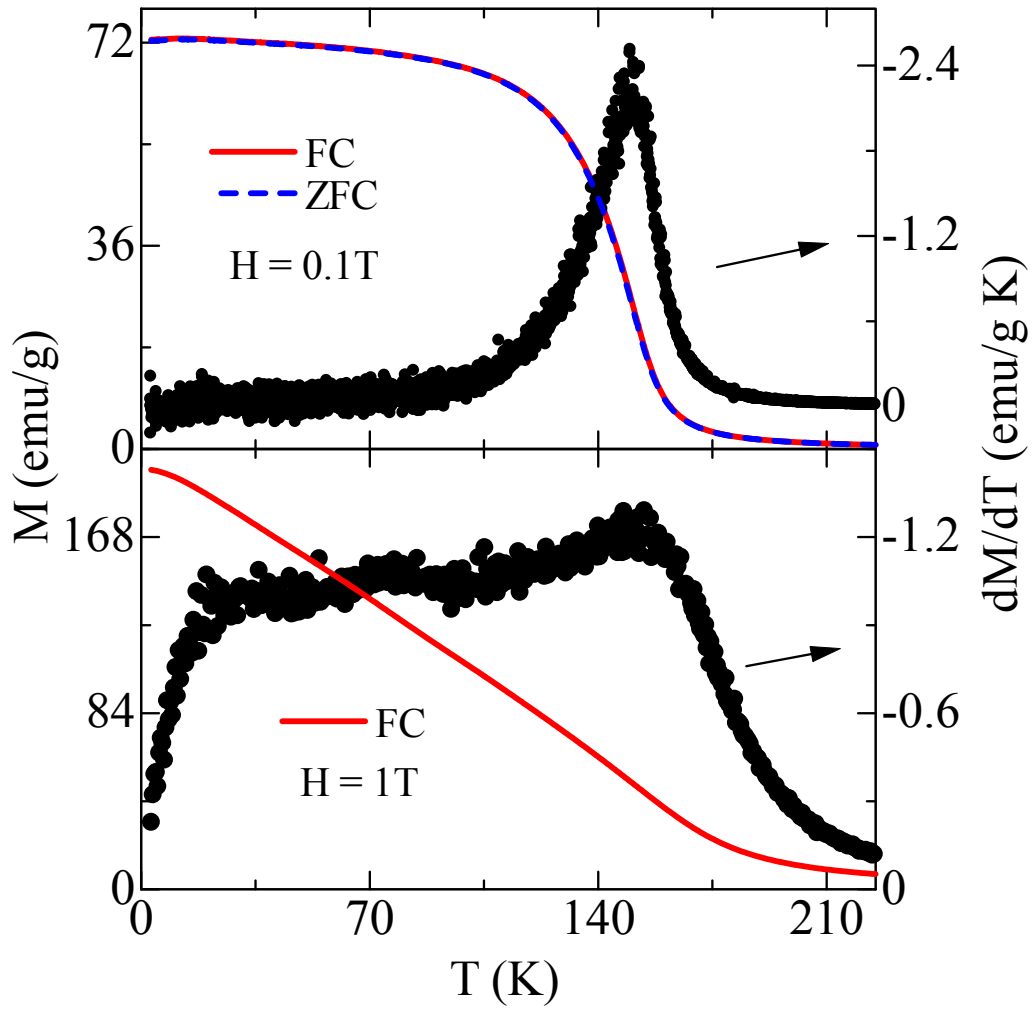


Fig. 9.

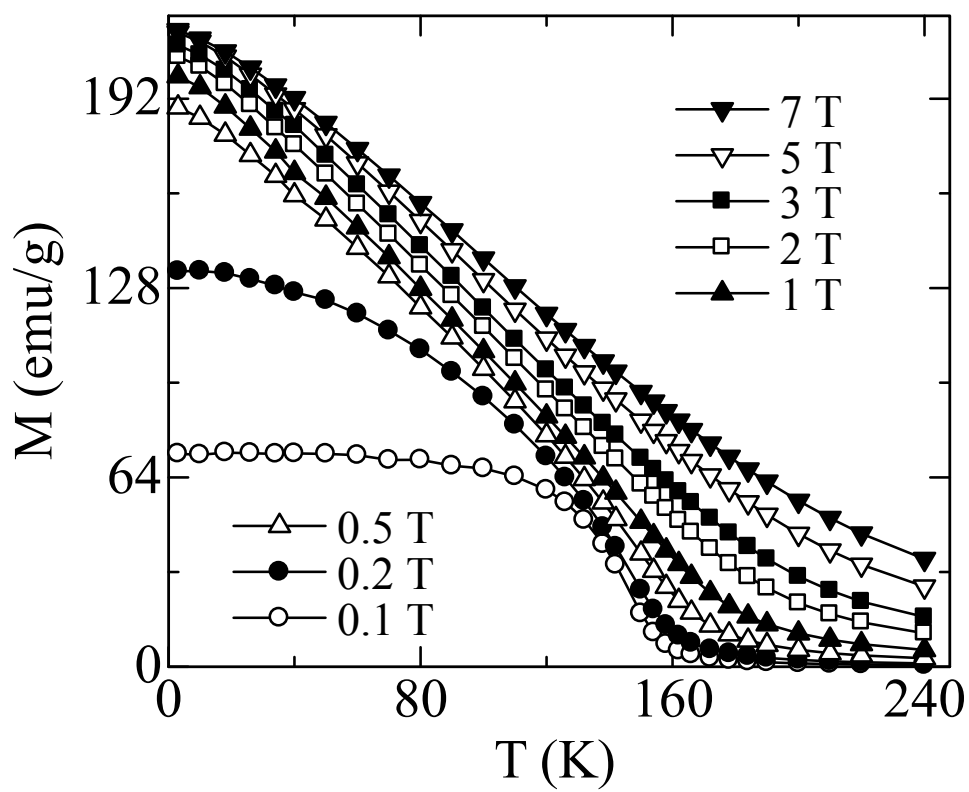


Fig. 10.

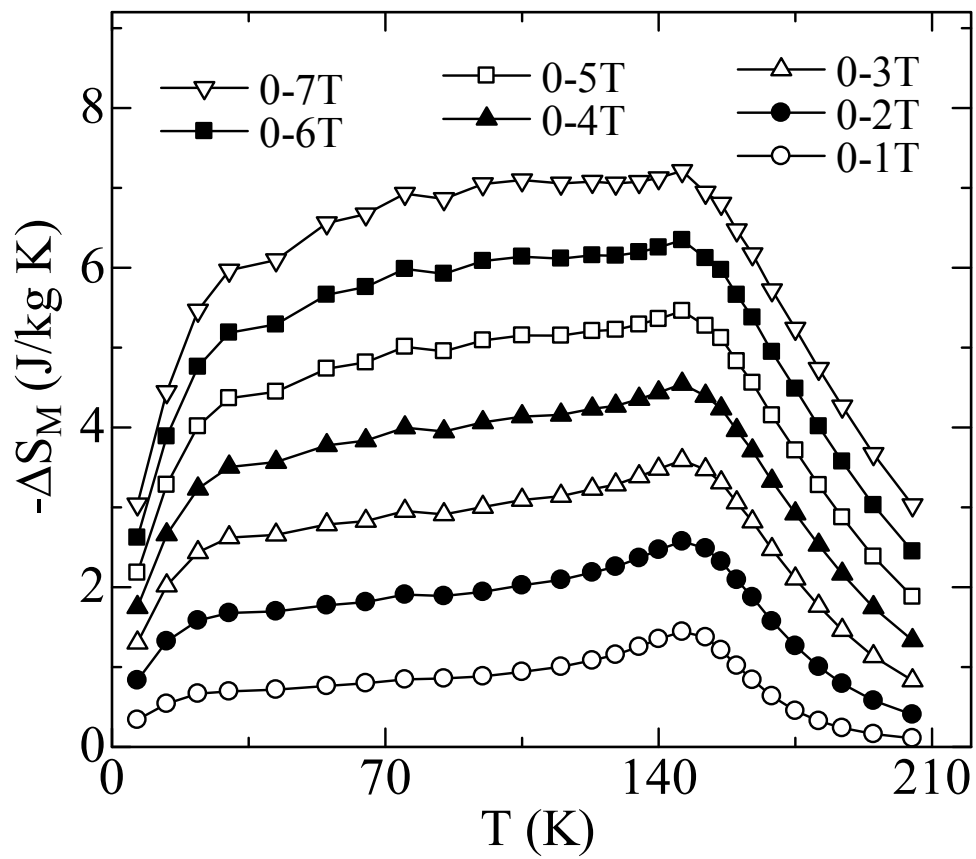


Fig. 11.

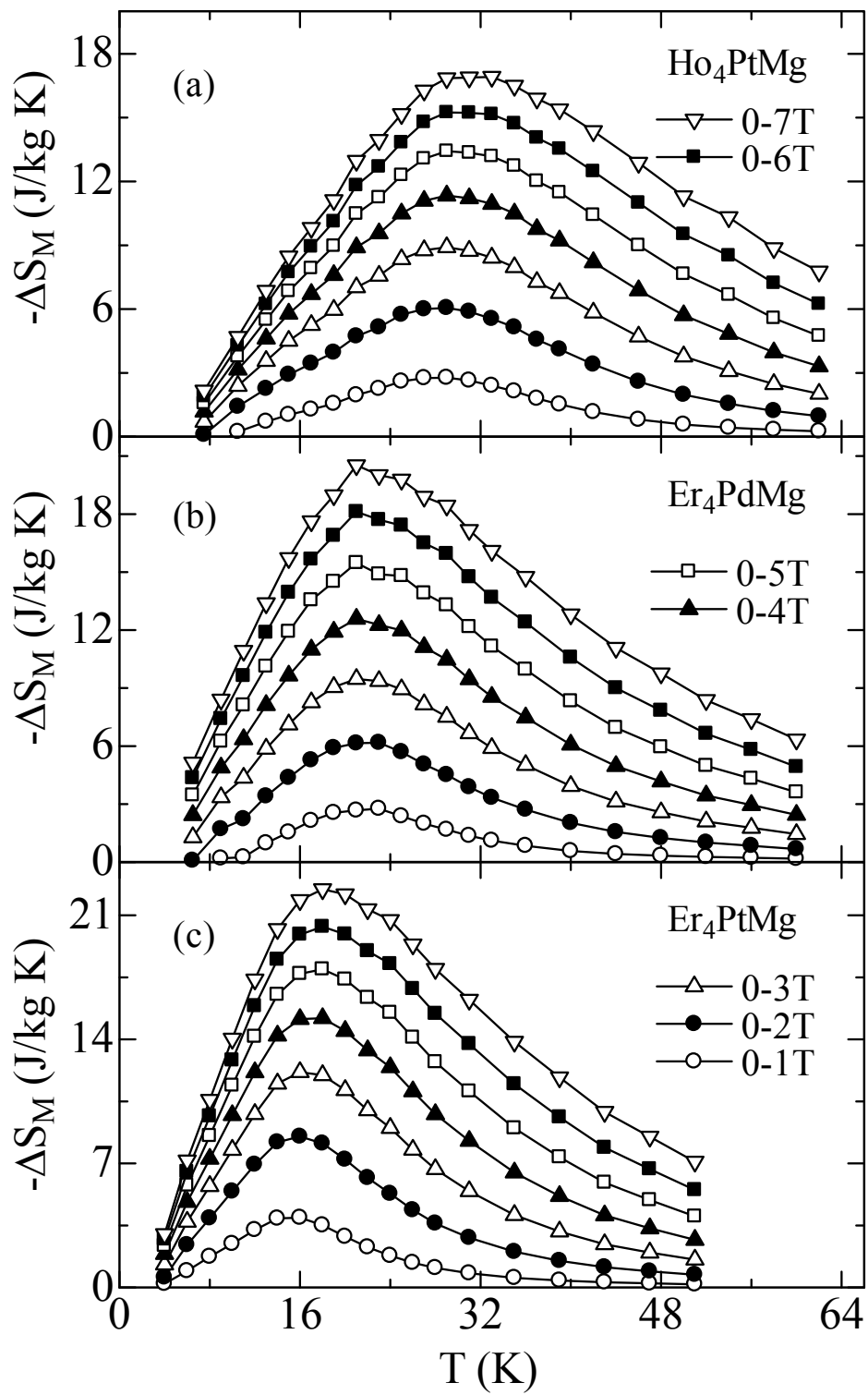


Fig. 12.

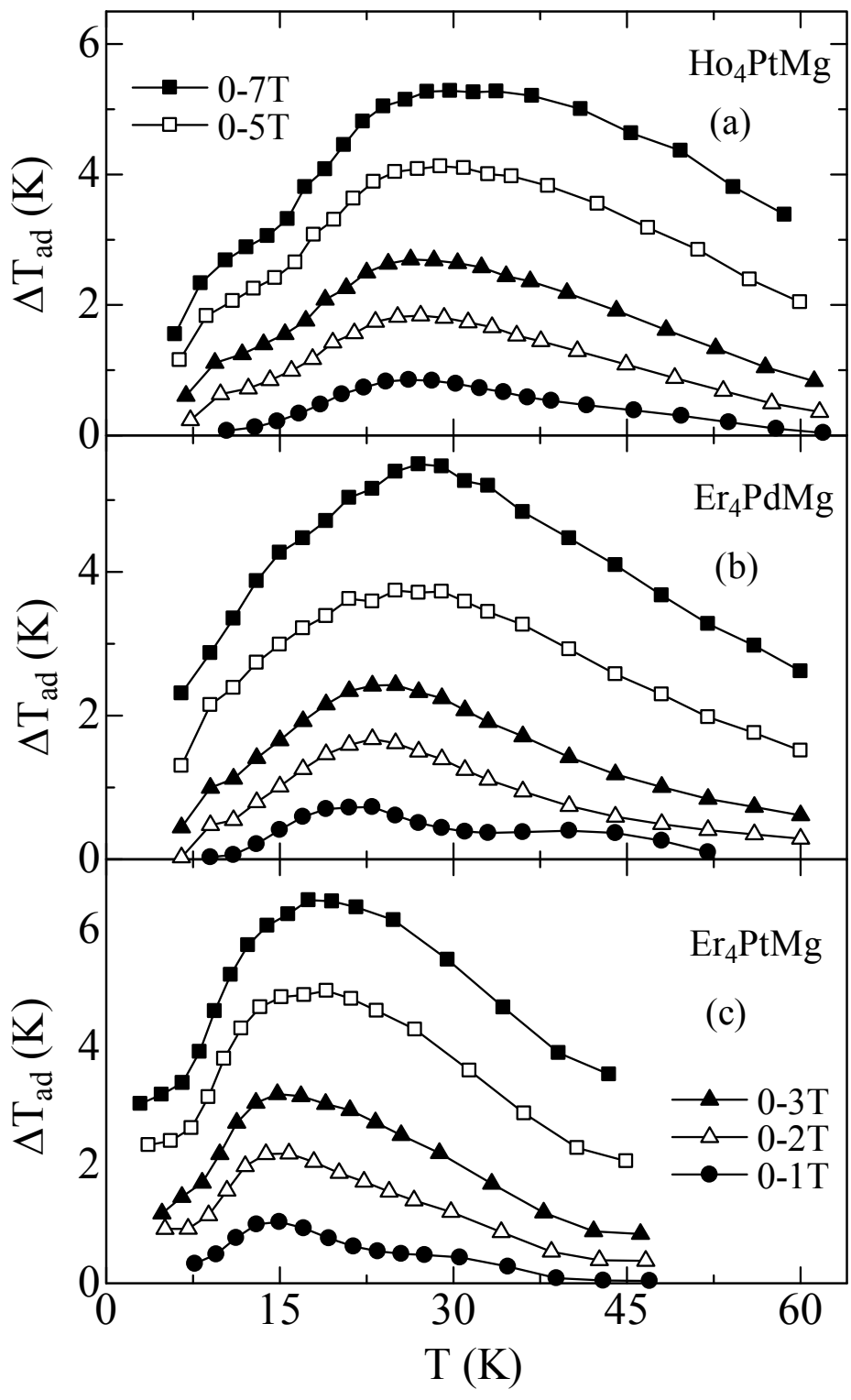


Fig. 13.

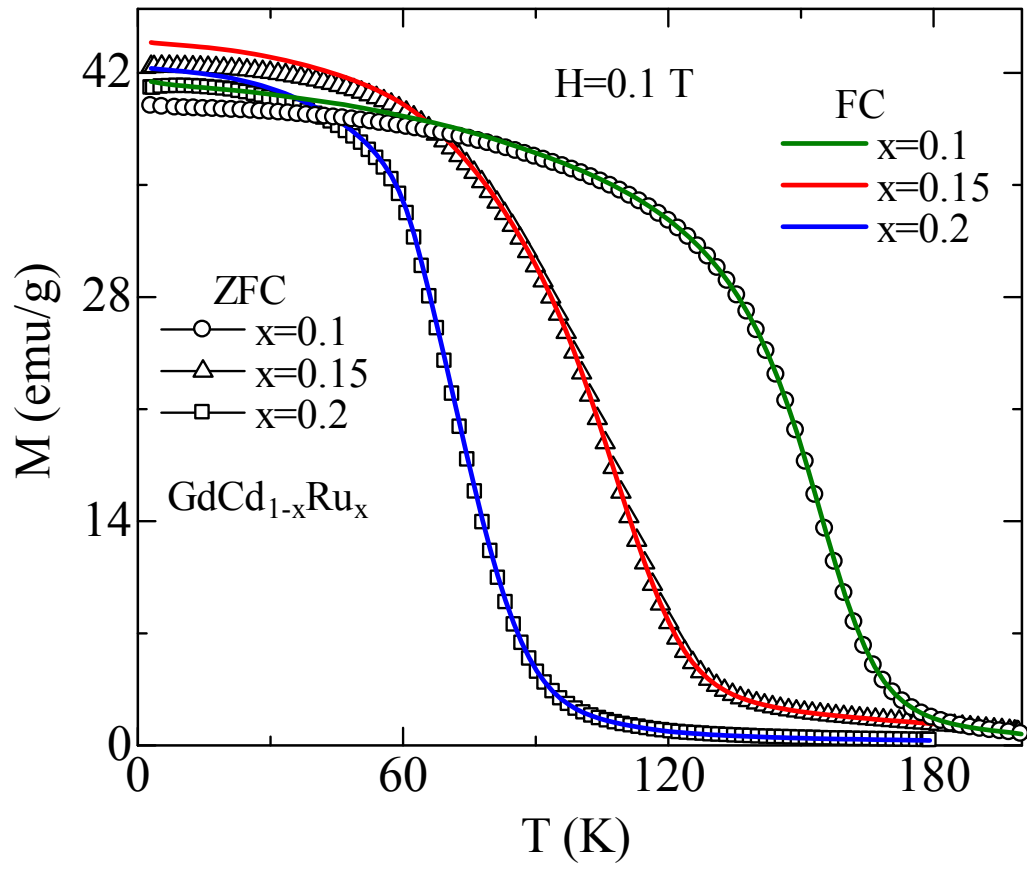


Fig. 14.

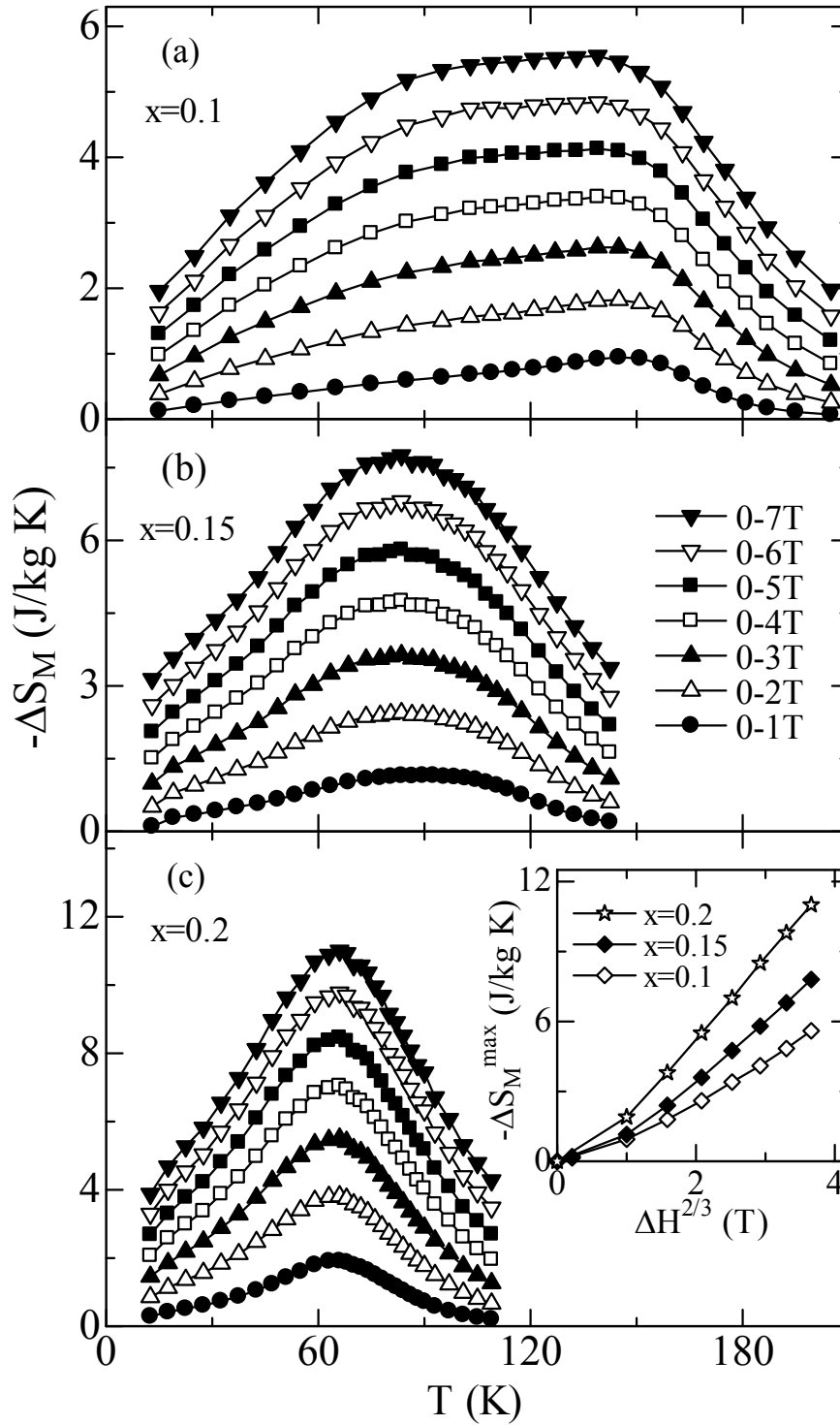


Fig. 15.

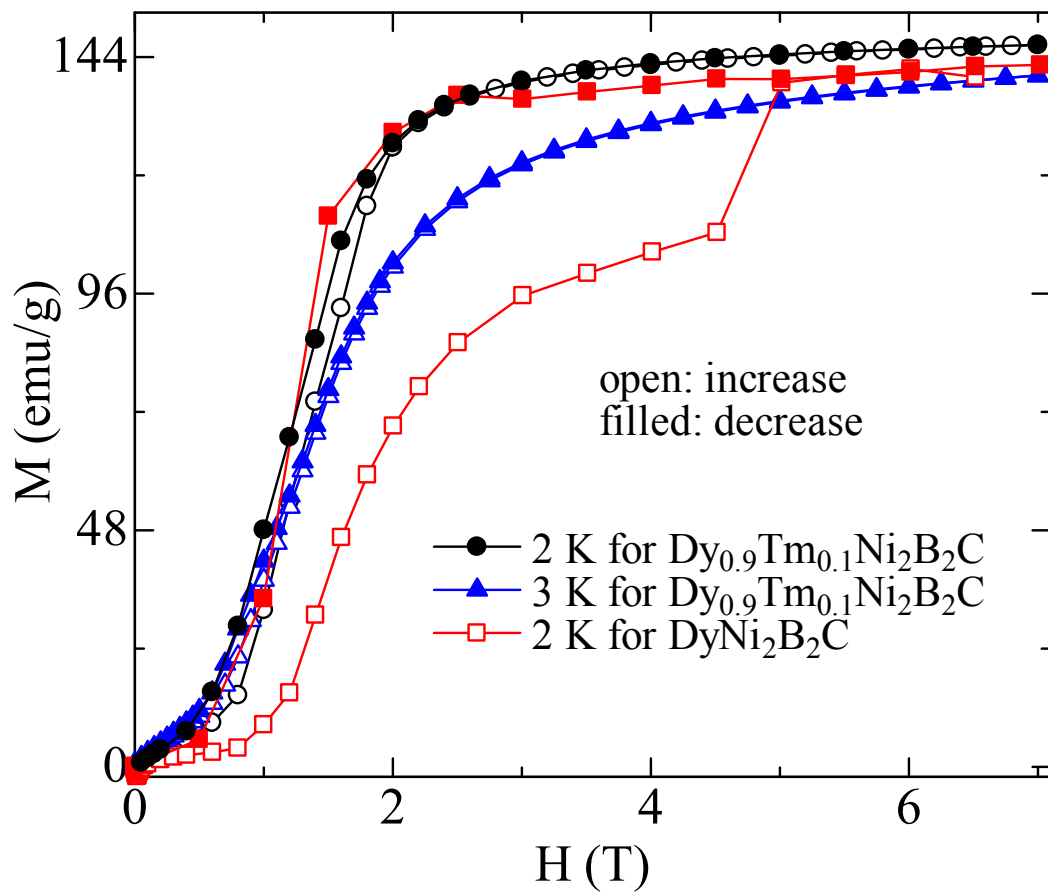


Fig. 16.

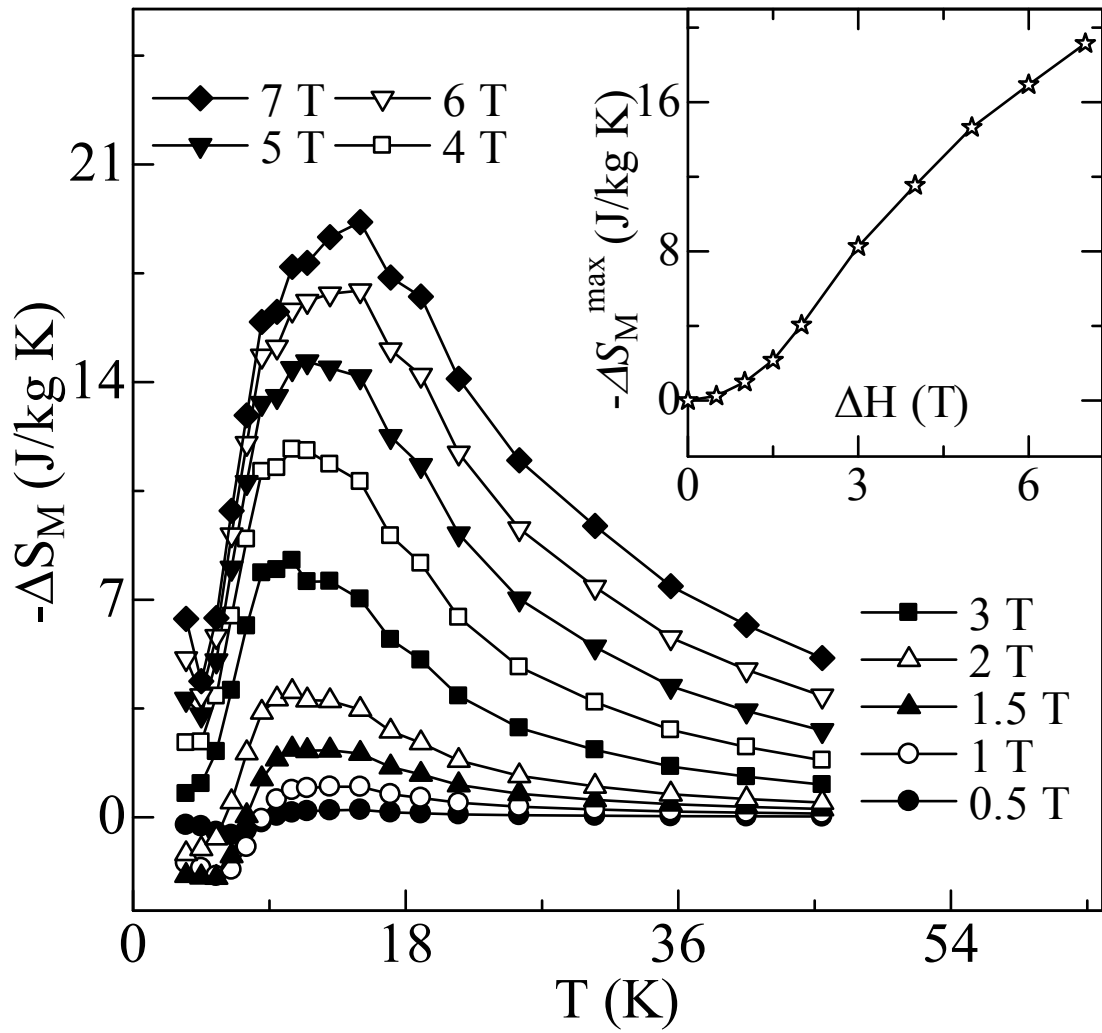


Fig. 17.

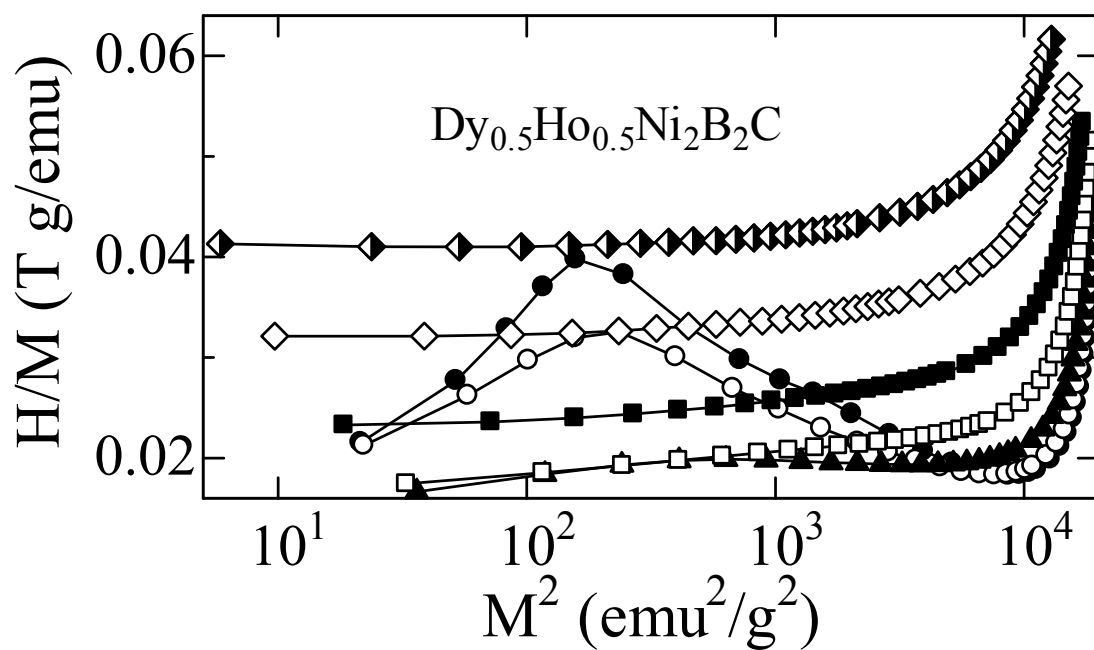
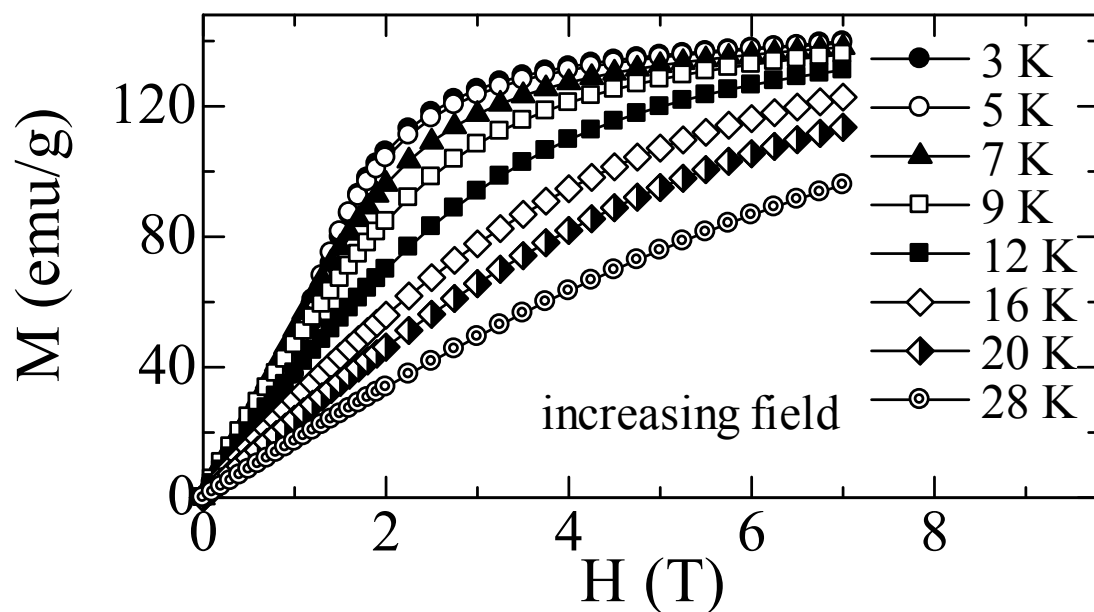


Fig. 18.

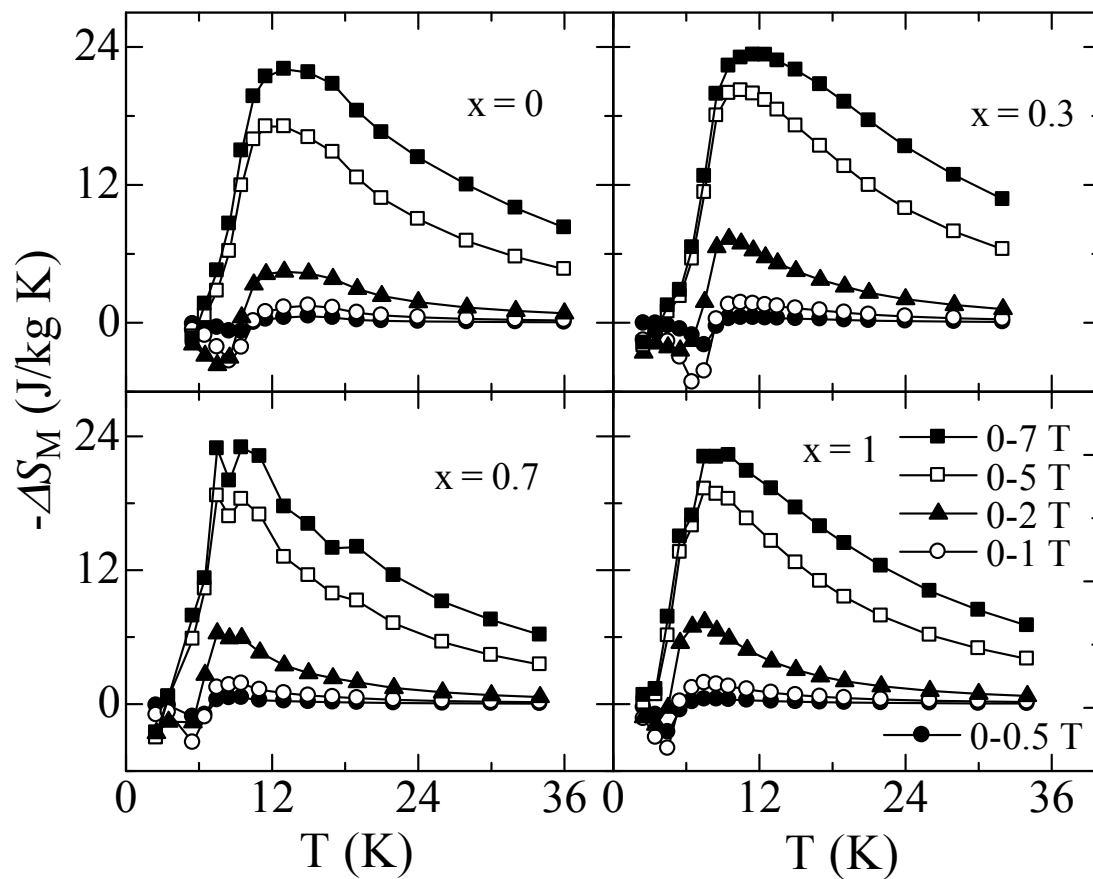


Fig. 19.

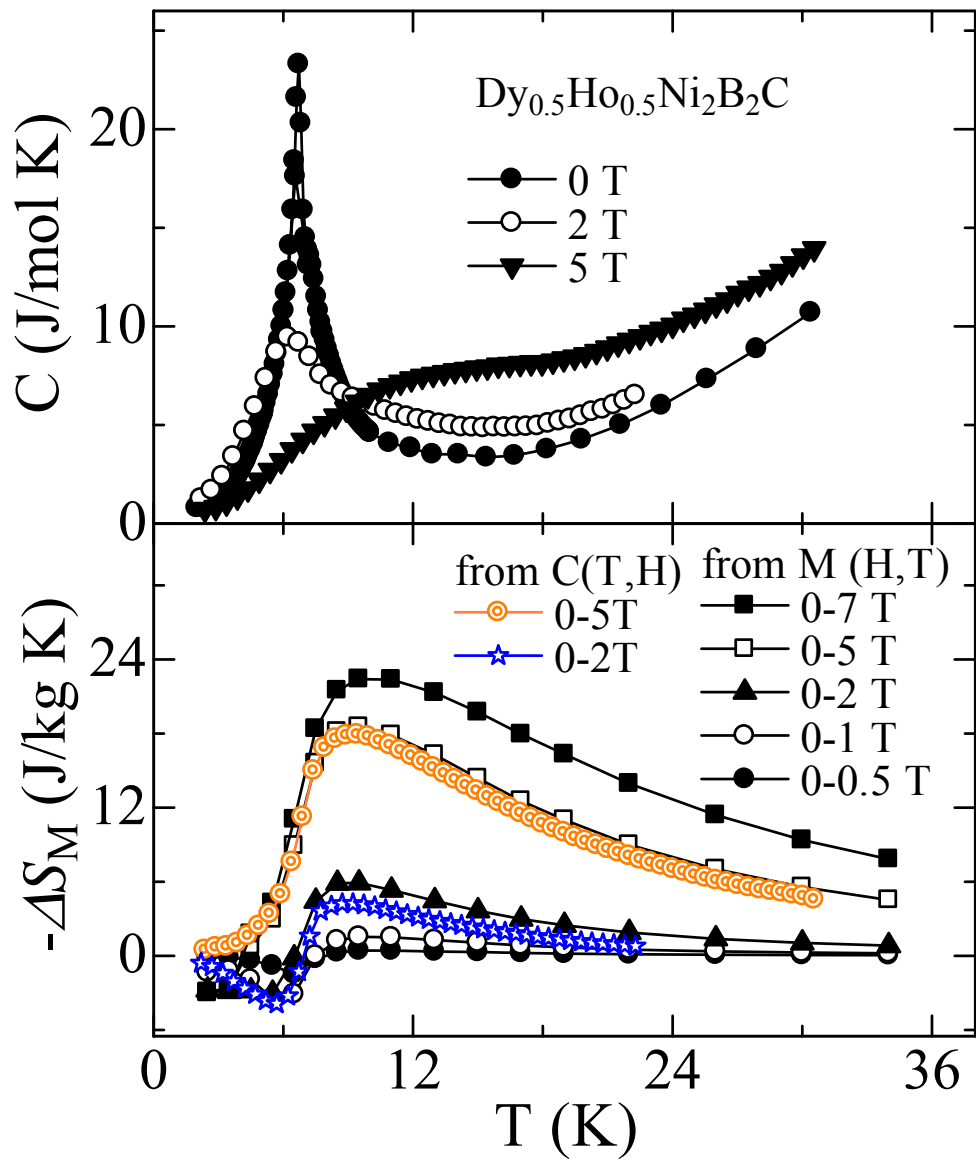


Fig. 20.

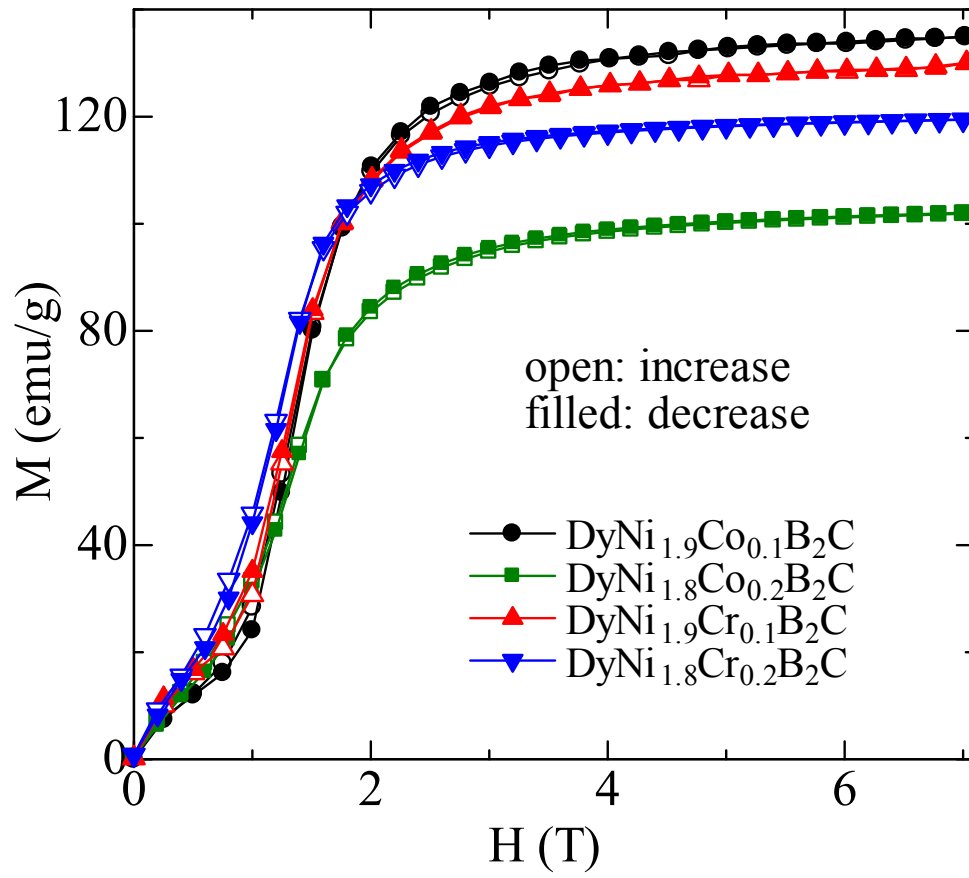


Fig. 21.

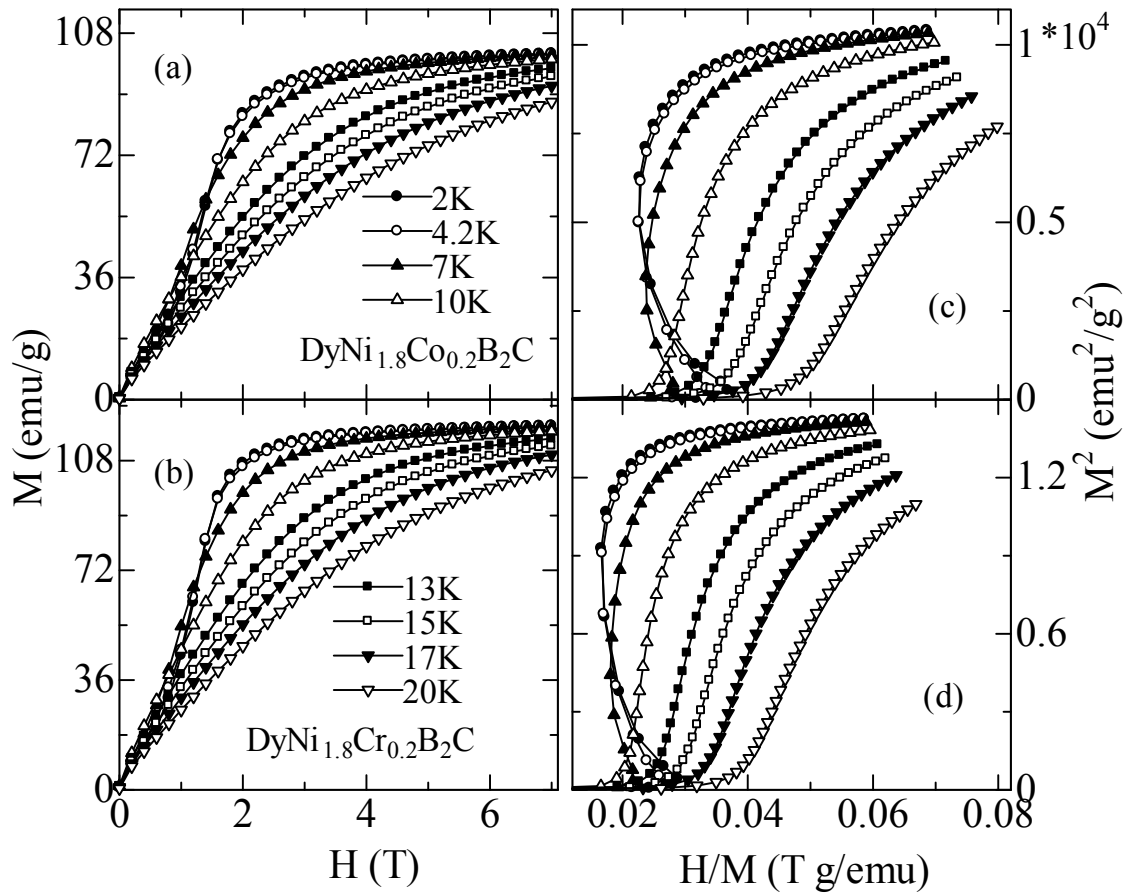


Fig. 22.

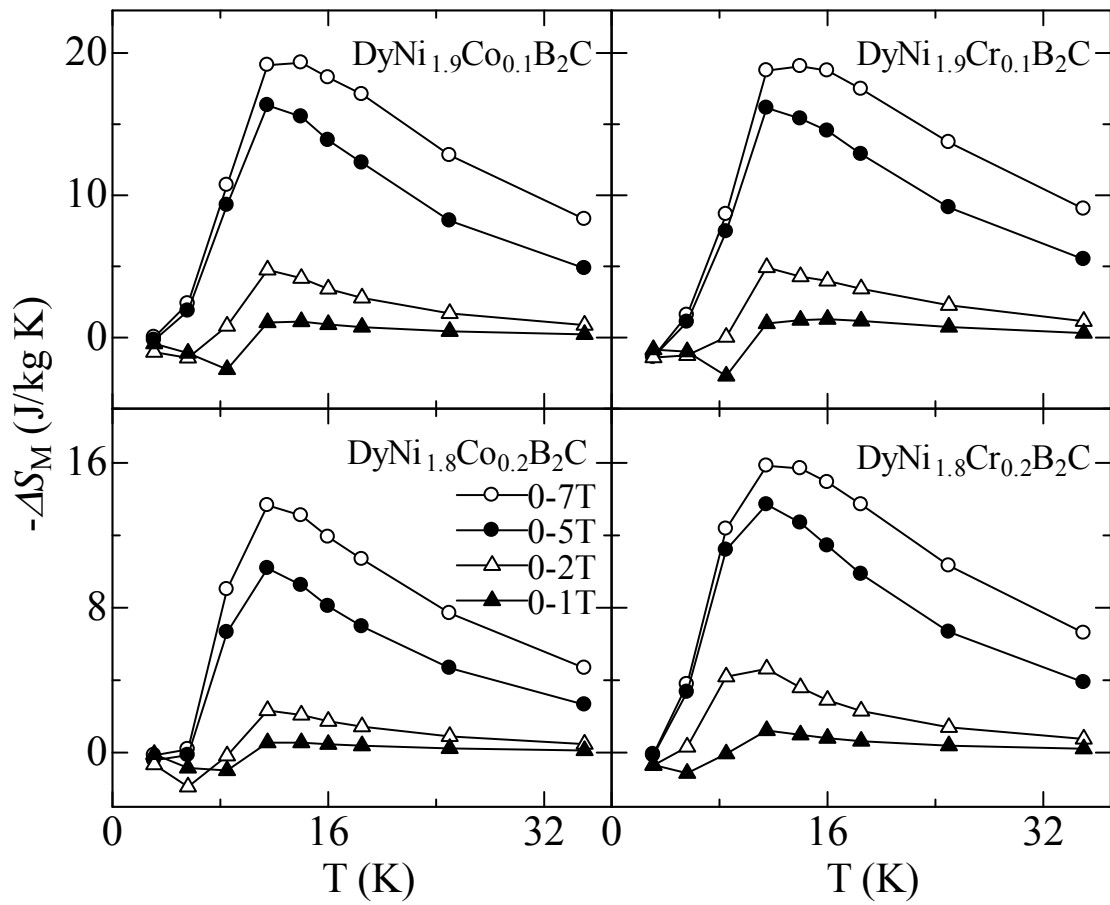


Fig. 23.

Table I. The transition temperature (T_M), the maximum magnetic entropy change ($-\Delta S_M^{\max}$), maximum adiabatic temperature change ($\Delta T_{\text{ad}}^{\max}$), and relative cooling power (RCP) under the field changes of 0-2 T and 0-5 T for the intermetallic compounds of rare earth with low boiling point metal(s) (Zn, Mg, and Cd) as well as some giant/large MCE materials with similar T_M .

The column with a mark "--" means that the value was not reported in the literature.

Compound	T_M (K)	$-\Delta S_M^{\max}$ (J/kg K)		RCP (J/kg)		$\Delta T_{\text{ad}}^{\max}$ (K)		Ref.
		2 T	5 T	2 T	5 T	2T	5T	
TmZn	8.4	19.6	26.9	76	269	3.3	8.6	57
HoZn	26/72	6.5	12.1	255	792	--	--	58
EuAuZn	51	4.8	9.1	105	318	--	--	59
EuRh _{1.2} Zn _{0.8}	95	3.1	5.7	233	513	1.4	2.8	60
TmZnAl	2.8	4.3	9.4	53	189	--	--	61
Eu ₄ PdMg	150	2.6	5.5	988	1346	--	--	66
Er ₄ PtMg	15	8.5	17.9	152	483	1.8	4.1	67
Er ₄ PdMg	21	6.2	15.5	142	457	1.7	3.7	68
Ho ₄ PtMg	28	6.1	13.4	177	527	2.2	5.0	67

Gd ₂ Ni _{0.5} Cu _{1.5} Mg	57	5.3	9.5	--	688	1.6	3.2	69
Gd ₂ NiCuMg	55.2	6.1	11.4	202	630	--	--	69
Gd ₄ Co ₂ Mg ₃	77	5.8	--	--	--	1.3	--	70
Er ₄ NiCd	5.9	7.3	18.3	237	595	3.1	7.7	72
GdCd _{0.9} Ru _{0.1}	149	1.8	4.1	235	636	--	--	73
GdCd _{0.85} Ru _{0.15}	108	2.4	5.8	223	597	--	--	73
GdCd _{0.8} Ru _{0.2}	73	3.8	8.5	213	583	--	--	73
ErCr ₂ Si ₂	1.9	24.1	29.7	136	388	8.4	17.4	76
TmAgAl	3.3	7.1	12.4	74	214	--	--	61
GdCr ₂ Si ₂	4.5	3.1	14.1	35	212	--	--	77
ErNiBC	5	17.1	24.8	155	312	5.3	8.6	78,79
TmMn ₂ Si ₂	5.5	15.3	22.7	106	250	5.0	10.1	80
ErMn ₂ Si ₂	6.5	20.0	25.2	130	365	5.4	12.9	81
Tm ₃ Co	8	11.6	19.9	93	300	--	--	82
HoCo ₂ B ₂	10	6.8	12.2	83	271	--	--	83
DyCo ₂ B ₂	10	5.4	12.1	88	282	--	--	83

ErAgAl	14	4.2	10.5	77	261	--	--	84
TbCo ₂ B ₂	15	1.5	6.2	49	292	--	--	83
GdNiBC	15	9.3	19.8	188	474	4.2	9.9	78,85
HoAgAl	18	3.8	10.3	99	344	--	--	84
DyCo ₃ B ₂	22	7.4	12.6	154	397	6.4	11.6	86
HoPdIn	6/23	7.9	14.6	112	496	2.6	5.5	87
GdCo ₂ B ₂	25	9.3	17.1	167	462	--	--	88
TbCo ₃ B ₂	28	4.9	8.7	59	295	4.0	7.3	89
NdMn ₂ Ge _{0.4} Si _{1.6}	36	12.3	28.4	95	284	2.1	4.1	90
GdCo ₃ B ₂	54	5.0	9.4	110	357	2.8	5.2	91
ErFeAl	55	2.4	6.1	77	311	--	--	92
DyFeSi	70	9.2	17.4	--	--	3.4	7.1	93
HoFeAl	80	3.4	7.5	174	563	--	--	92
Ho ₂ In	85	--	11.2	--	360	--	--	94
Gd ₅₃ Al ₂₄ Co ₂₀ Zr ₃ (micro-wire)	96	--	10.3	--	733	--	--	95
Gd ₅₅ Al ₂₀ Co ₂₀ Ni ₅	105	6.59	9.8	--	829	--	4.74	96

(metallic glass)

DyFeAl	126	3.1	6.4	190	595	--	--	97
Gd ₅ Ir ₂ Sn	154	3.9	7.3	176	423	--	--	98

Table II. The superconductivity transition temperature (T_{SC}), magnetic transition temperature (T_M), the maximum values of magnetocaloric parameters ($-\Delta S_M^{\max}$ and ΔT_{ad}) as well as the relative cooling power (RCP) for the magnetic field change of 0-5 T in the rare earth nickel boroncarbides $RENi_2B_2C$ and $RENiBC$ compounds.

The column with a mark “--” means that the value was not reported in the literature.

The column with a mark “N” means that superconductivity was not observed above 2 K.

Material	T_{SC} (K)	T_M (K)	$-\Delta S_M^{\max}$ (J/kg K)	ΔT_{ad}^{\max} (K)	RCP (J/kg)	Reference
Dy _{0.9} Tm _{0.1} Ni ₂ B ₂ C	4.5	9.2	14.7	--	248	104
HoNi ₂ B ₂ C	8.2	5	17.7/19.2	11	283	105,106
Dy _{0.3} Ho _{0.7} Ni ₂ B ₂ C	8.1	6	18.7	--	264	106
Dy _{0.5} Ho _{0.5} Ni ₂ B ₂ C	6.2	8	18.5	--	275	106

Dy _{0.7} Ho _{0.3} Ni ₂ B ₂ C	6.4	8.5	20.2	--	243	106
DyNi ₂ B ₂ C	6.4	10.5	17.6/17.1	9.7	290	105,106
DyNi _{1.9} Co _{0.1} B ₂ C	N	8.4	16.3	--	309	107
DyNi _{1.9} Co _{0.2} B ₂ C	N	8	10.2	--	168	107
DyNi _{1.9} Cr _{0.1} B ₂ C	N	9.2	16.1	--	272	107
DyNi _{1.9} Cr _{0.2} B ₂ C	N	8.8	13.7	--	219	107
ErNi ₂ B ₂ C	10.5	6.1	11.1/9.8	4.6	155	105,108
ErNi _{1.9} Fe _{0.1} B ₂ C	N	5.6	9.6	--	106	108
ErNi _{1.9} Fe _{0.2} B ₂ C	N	5.2	8.0	--	71	108
